

# Forbush Decreases: The View From Space

Ian G. Richardson

CRESST/Department of Astronomy,  
University of Maryland, College Park, and  
Astroparticle Physics Laboratory, Code 661  
NASA Goddard Space Flight Center

With thanks to Hilary Cane (University of Tasmania),  
Gerd Wibberenz (U. of Kiel) and Tycho von Roseninge (GSFC)

# Forbush Decrease – Short-term (<~few days duration) depression in the Galactic Cosmic Ray intensity

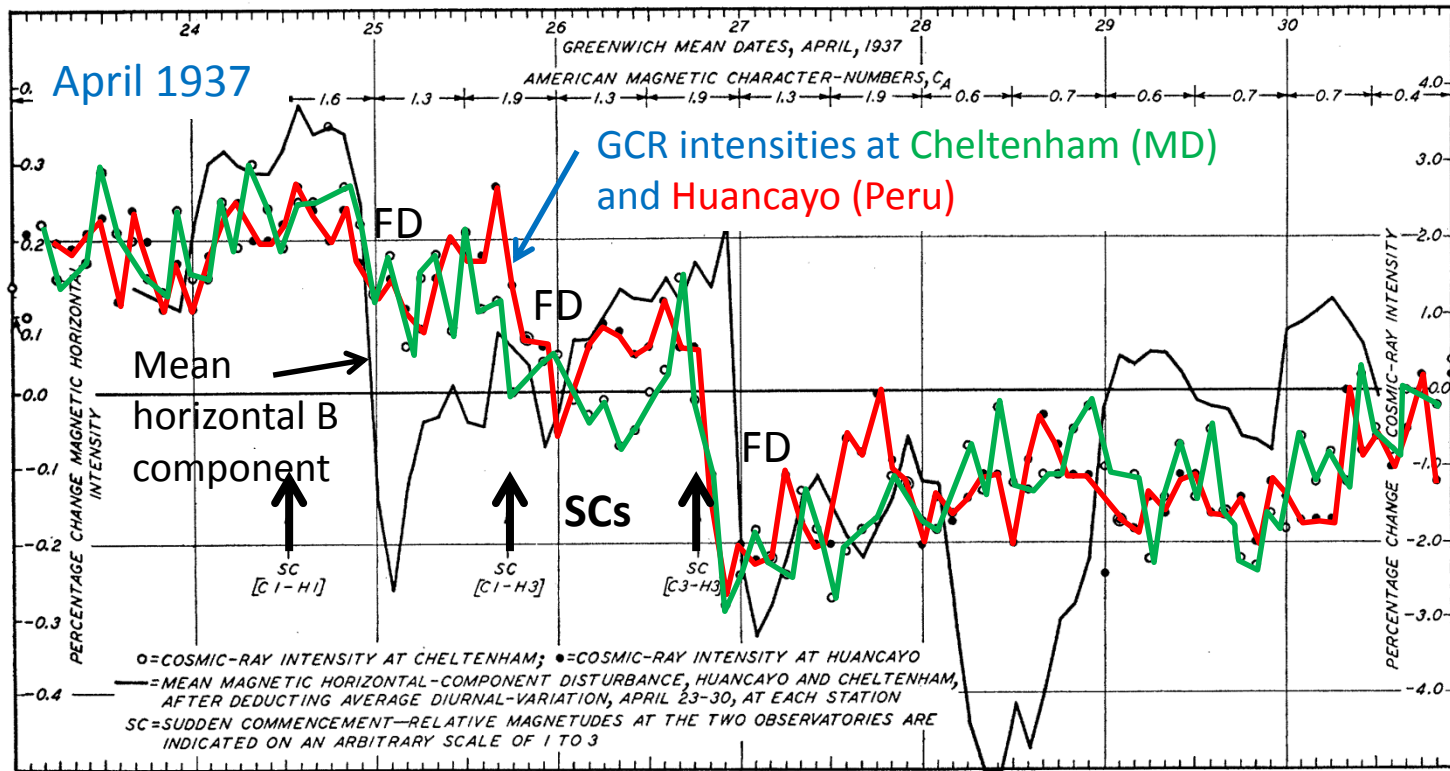


FIG. 1. Bi-hourly departures expressed in percentage of absolute values for cosmic-ray intensity and for disturbance of horizontal magnetic component April 23-30, 1937, Huancayo and Cheltenham magnetic observatories.

Scott E. Forbush  
1904-1984



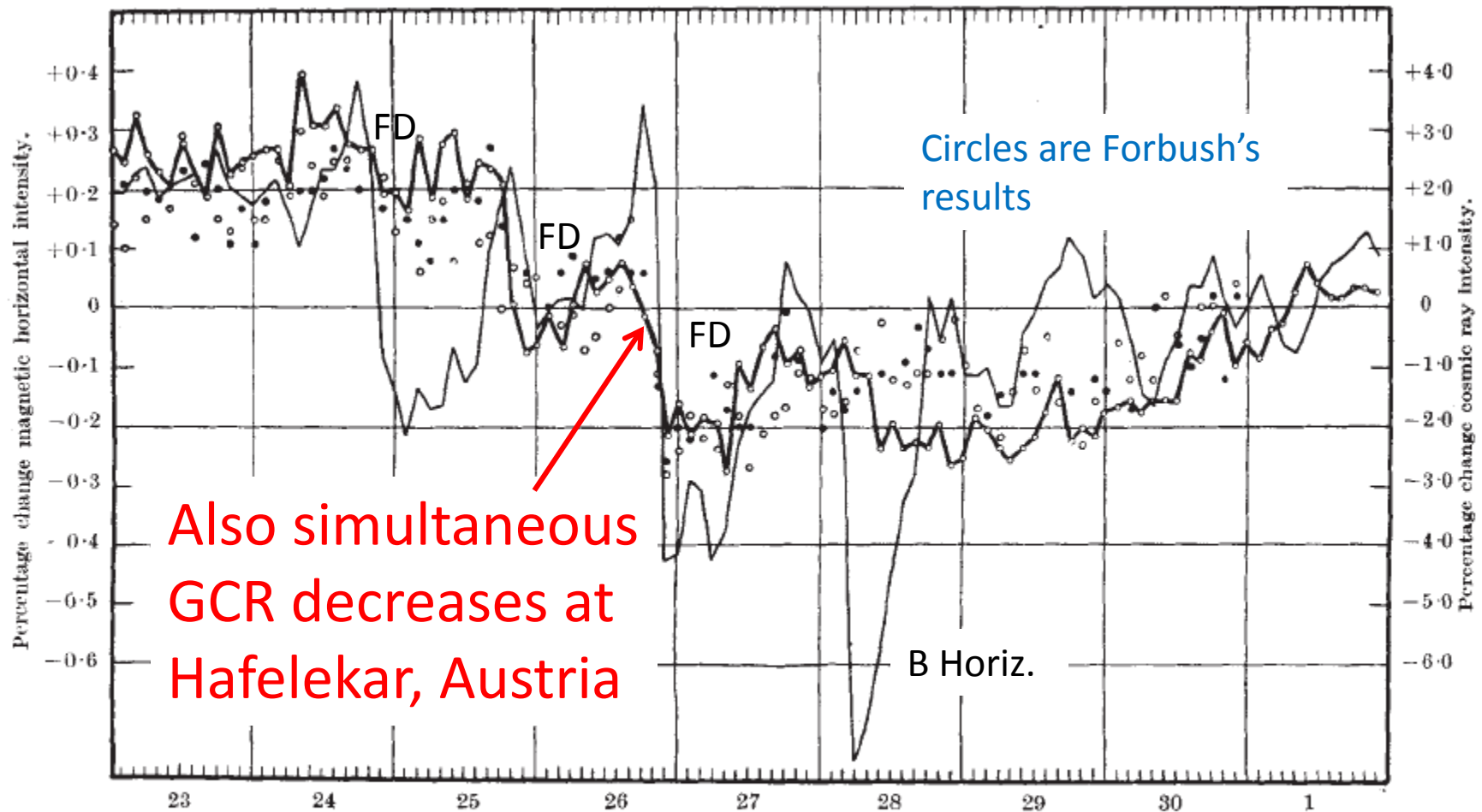
From  
obituary in  
Physics Today

Simultaneous GCR decreases (~3%) measured by ionization chambers in Maryland and Peru  
=> Worldwide Phenomenon

Closely associated with geomagnetic storm sudden commencements => External driver

Forbush, S.E.: 1937, *Phys. Rev.* **51**, 1108.

Also Hess and Demmelmair, 1937, Nature 140, 316.



Also simultaneous  
GCR decreases at  
Hafelekar, Austria

FIG. 1.

BI-HOURLY MEAN VALUES OF COSMIC RAY INTENSITY AND OF MAGNETIC HORIZONTAL INTENSITY,  
APRIL 23 TO MAY 1, 1937.

, Cosmic ray intensity, Huancayo. o, Cosmic ray intensity, Cheltenham. o—o—o, Cosmic ray intensity, Hafelekar.

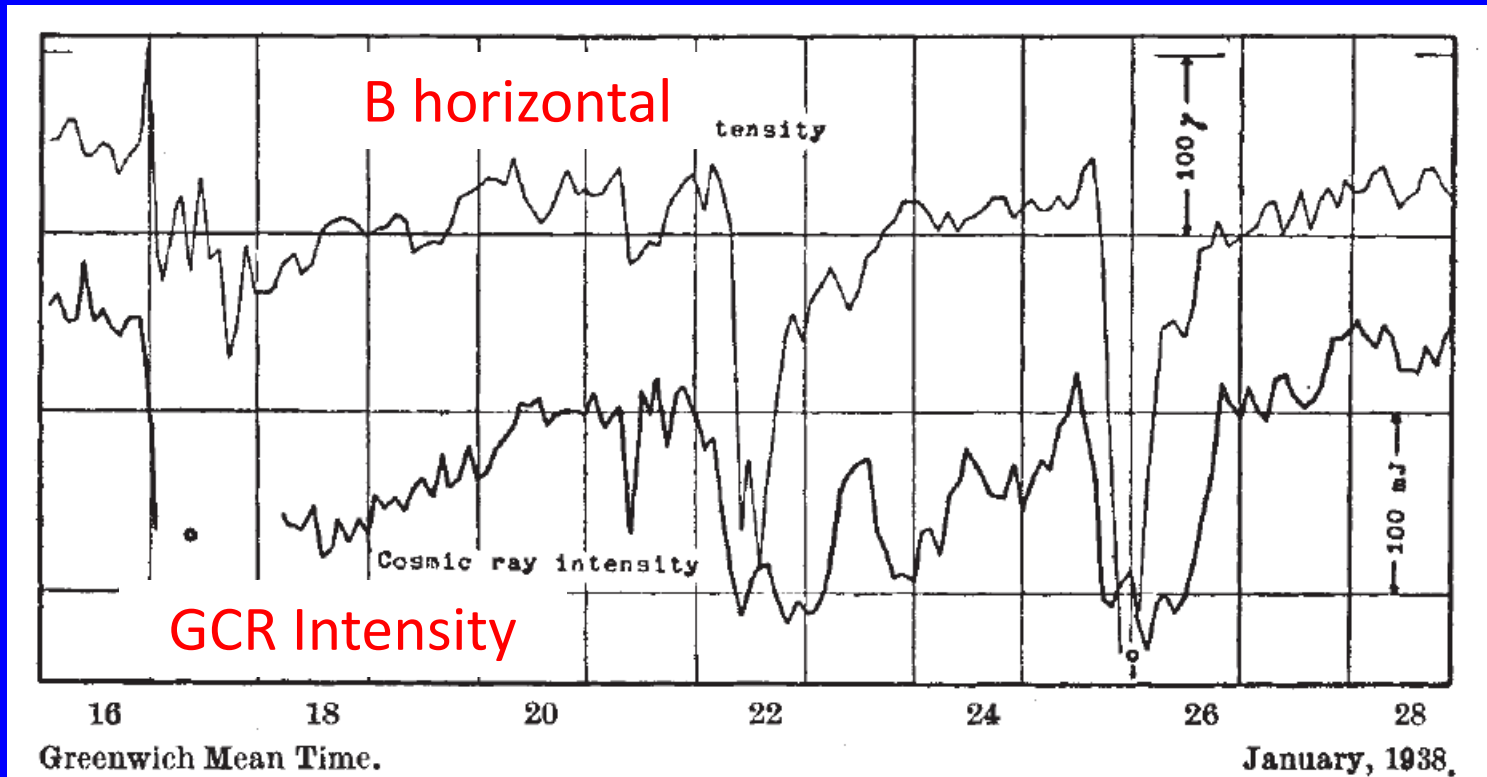


Fig. 1.

TWO-HOUR MEAN VALUES OF THE MAGNETIC HORIZONTAL INTENSITY AND OF THE COSMIC RAY IONIZATION DURING THE MAGNETIC AND AURORAL DISTURBANCES OF JANUARY 16-28, 1938. AVERAGE COSMIC RAY INTENSITY, 2356 mJ. AVERAGE HORIZONTAL INTENSITY 20,432  $\gamma$ .

- Correlation between GCR intensity and B horizontal (ring current)
- Ring current reduces Bhorizontal at the Earth's surface (Chapman, 1937) but increases the dipole moment of the Earth => reduces the measured GCR intensity.

# Discovery of Solar Energetic Particle (SEP) Events (*Forbush, 1946*)

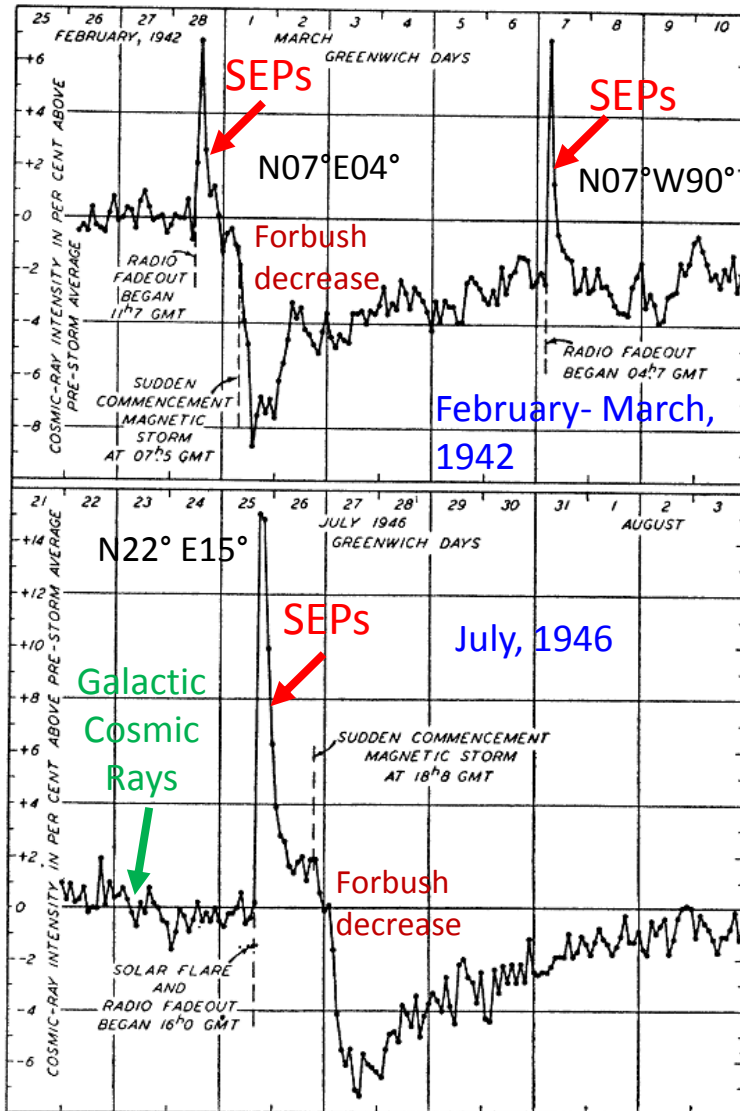


FIG. 1. Three unusual increases in cosmic-ray intensity at Cheltenham, Maryland, during solar flares and radio fadeouts.

## Three Unusual Cosmic-Ray Increases Possibly Due to Charged Particles from the Sun

SCOTT E. FORBUSH

Department of Terrestrial Magnetism,  
Carnegie Institution of Washington, Washington, D. C.

October 10, 1946

Began ~simultaneously with (< 1 hour after) a solar flare or radio fade out indicating a flare.

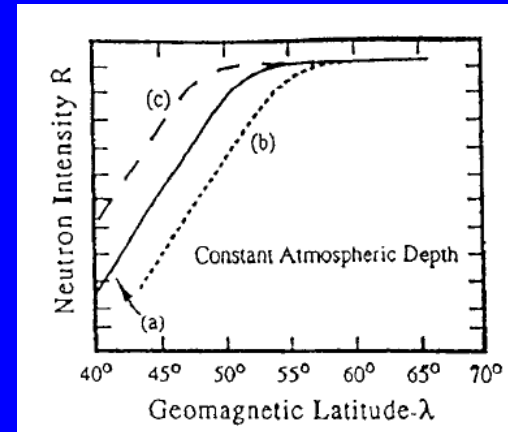
These considerations suggest the rather striking possibility that the three unusual increases in cosmic-ray intensity may have been caused by charged particles actually being emitted by the Sun with sufficient energy to reach the Earth at geomagnetic latitude 48° but not at the equator. It is recognized that particles of this energy should not escape from low latitudes on the Sun except in the absence of the much-disputed permanent solar magnetic field.

But interpreted as evidence of the absence of a permanent solar magnetic field!

(Flare locations from *Shea and Smart, 1991*)

# Forbush Decreases are an Interplanetary, not a Local, Phenomenon

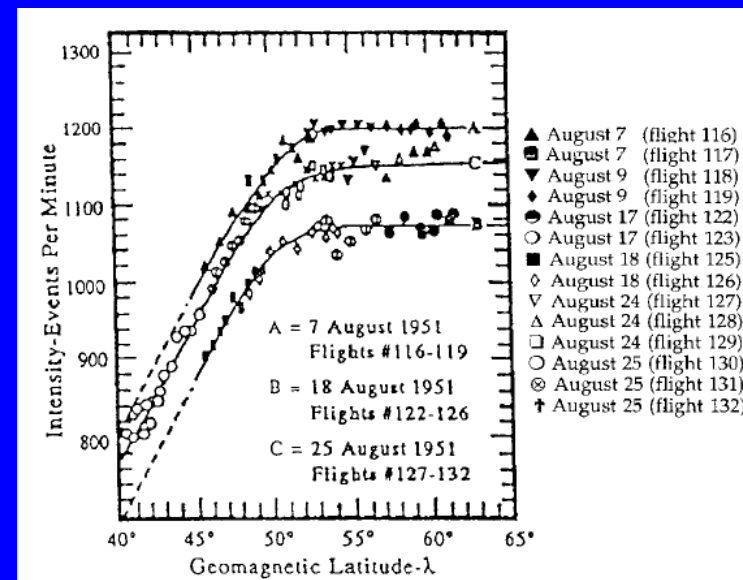
Expected: Enhancement in geomagnetic cut off – no change in intensity at high geomagnetic latitudes



Observed: Intensity variations at all geomagnetic latitudes, no change in cut off (*Meyer and Simpson, 1955; Simpson, 2000*)



John Simpson mounted a small neutron monitor in the nose of a jet aircraft.



# Early Concepts of Mass Ejections From The Sun

Lindeman 1919



Chapman Ferraro 1929

Magnetized Plasma Clouds

Beam & Frozen-in Fields



Alfvén 1954

Turbulent Cloud



Morrison 1956

Tongue



Cocconi et al. 1958

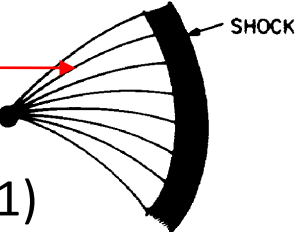
Bottle; Bubble



Piddington 1958

Shock Wave

Blast Wave, no driver/ICME



Parker 1961

(Burlaga, 1991)

Pre-Solar Wind



- Inferred from e.g.:
- Geomagnetic storms several days after solar flares/ eruptions;
- Galactic cosmic ray (Forbush) decreases;
- Abrupt geomagnetic storm onsets => arrival of shocks *Gold, 1955*);

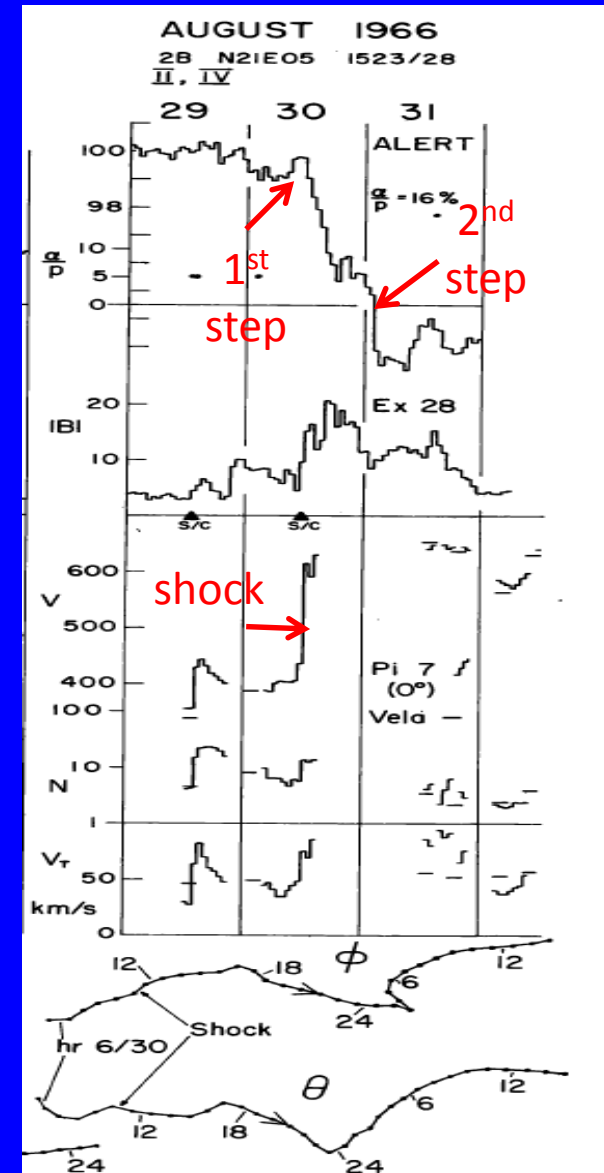
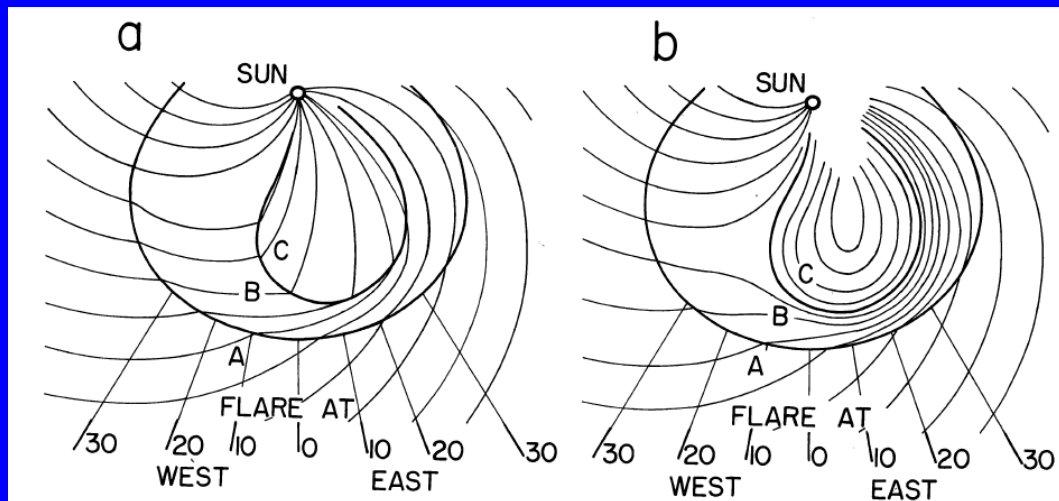
# L. R. Barnden "The Large-Scale Magnetic Field Configuration Associated With Forbush Decreases", Proc. 13<sup>th</sup> ICRC, 1973

Studied two step FDs.

- First step associated with shock arrival

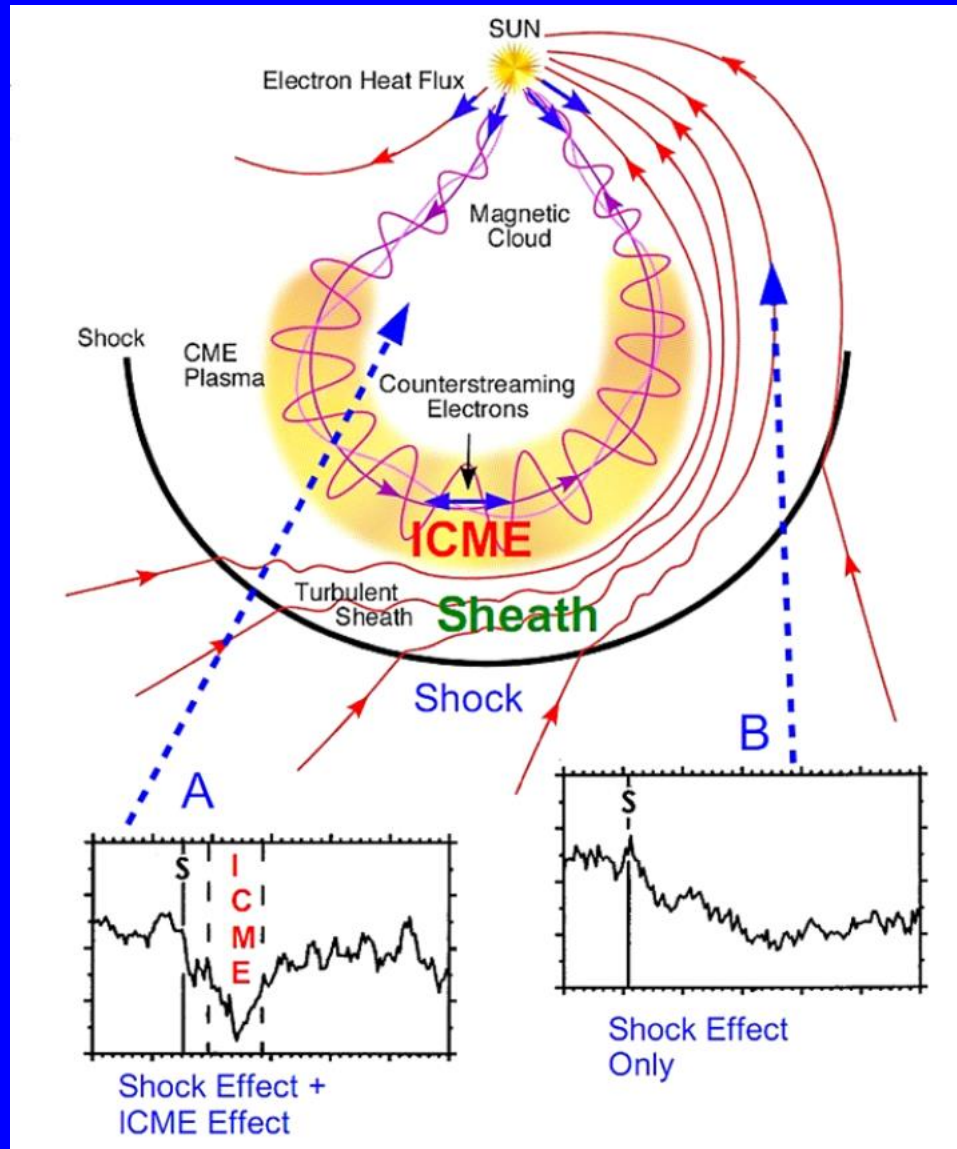
- Second step associated with entry into "bottle-like" magnetic field configuration:

- Perpendicular diffusion is slow, so particle movement into the bottle is restricted;
- Sharp drop in GCR and shock-accelerated particles at bottle boundary consistent with tangential discontinuity
- Field-aligned bidirectional GCR flows in bottle.





# Schematic of GCR Variations Along Two Trajectories Through a Shock and ICME



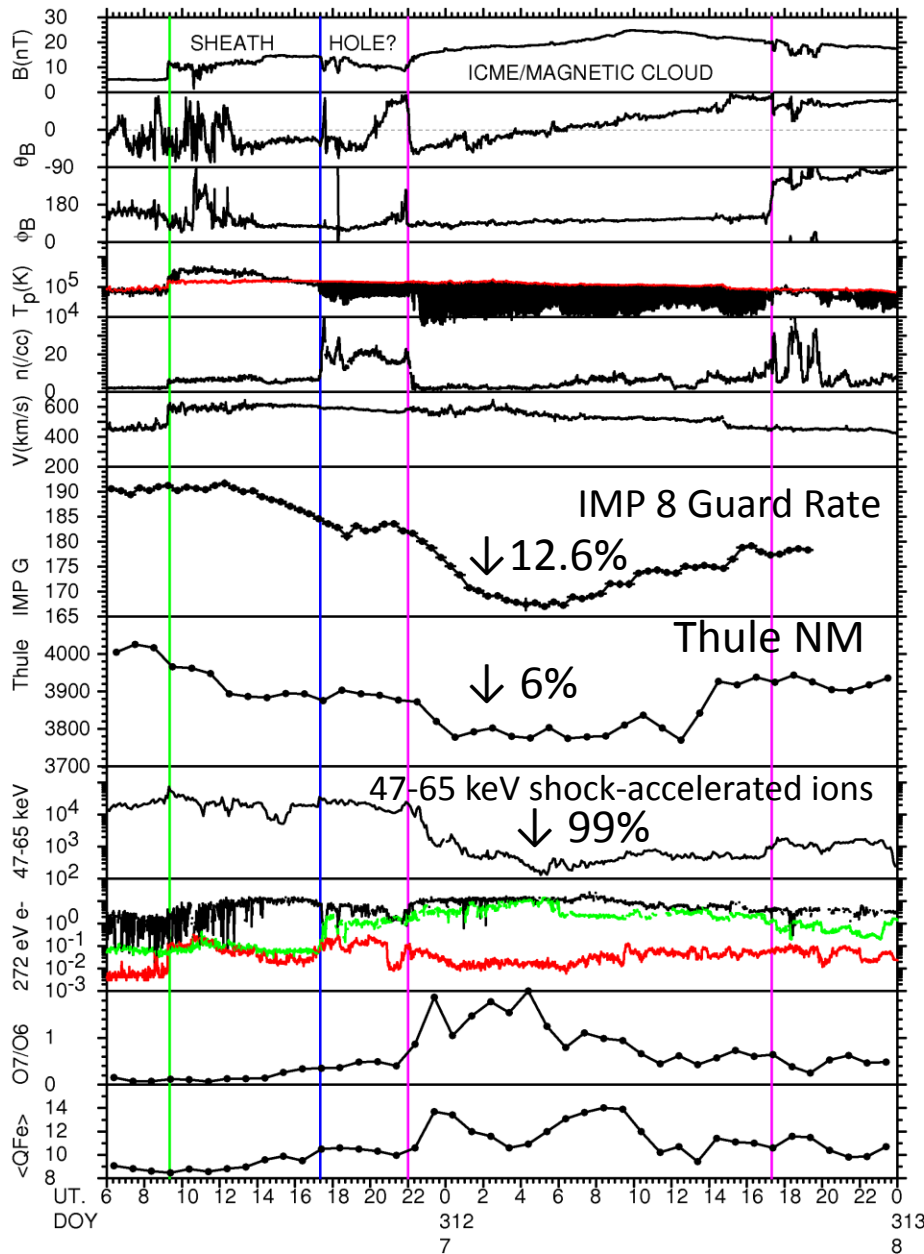
# Solar Wind Observations Associated with a Two- Step FD in November 2000

First GCR step is in sheath between shock and ICME (a “magnetic cloud” with an enhanced magnetic field which rotates slowly in direction suggestive of a flux rope structure.

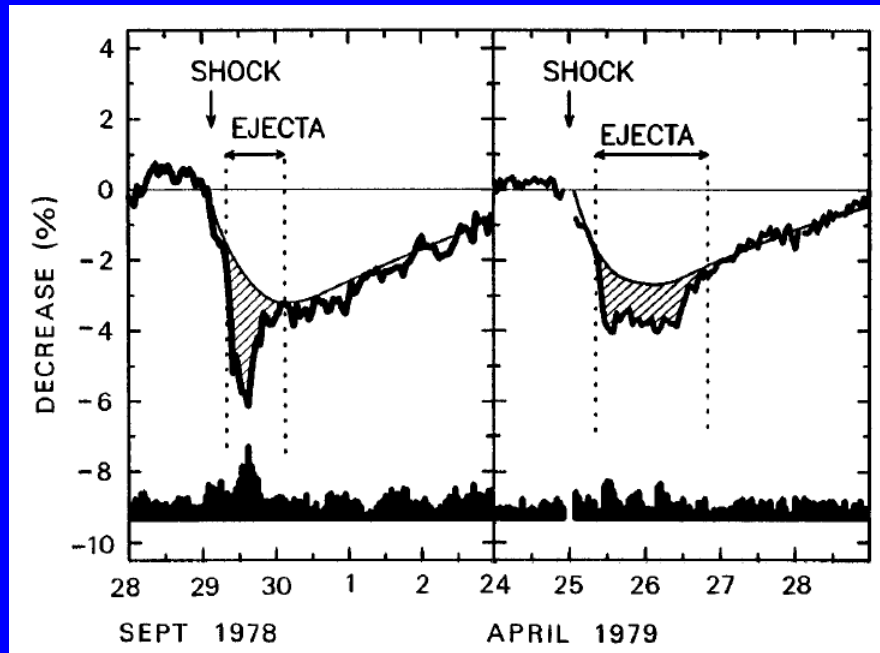
Second GCR step commences on ICME entry; maximum GCR depression is in the ICME.

Note also decrease in shock-accelerated ions at ICME entry.

ICME is also characterized by enhanced solar wind ion charge states and bidirectional suprathermal electron flows



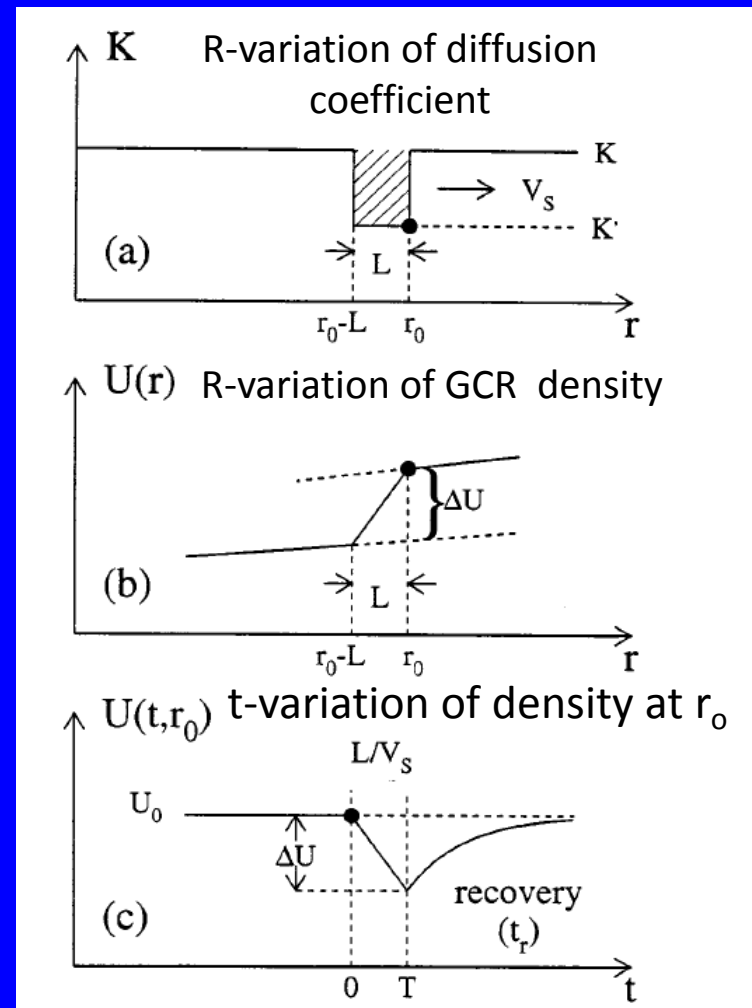
# Propagating Diffusive Barrier Model for Shock Effect (*Wibberenz et al., 1998*)



$$\frac{\Delta U}{U_o} = G_r L \left( \frac{V'}{V} \cdot \frac{B'^2}{B^2} \cdot \frac{K_{||}}{K'_{||}} - 1 \right) \quad \Leftarrow$$

' = downstream values

$G_r$  = upstream GCR radial gradient



# “Heat conduction” Model for the Ejecta Effect (Cane et al., 1995, Vanhoefer, 1996)

Assume:

A cylindrical ejecta that does not change shape or size during propagation at a constant speed  $V$  away from the Sun.

Particles diffuse into the ejecta

$$\Rightarrow \frac{\Delta U}{U_0} = F \left( \frac{K_{\perp} r}{V a^2} \right)$$

Where  $K_{\text{perp}}$  is the perpendicular diffusion coefficient;

$r$  = distance from Sun;

$a$  = ejecta radius;

$V$  = ejecta speed.

If  $K_{\text{perp}} \propto 1/B$ , then  $\Delta U/U_0 \sim Ba^2V$

$\Rightarrow$  Larger  $Fd$  if  $B$ , ejecta size or speed are increased.

# Effect of Finite Larmor Radius on Cosmic-ray Penetration into an Interplanetary Magnetic Flux Rope (*Kubo and Shimazu, 2010*)

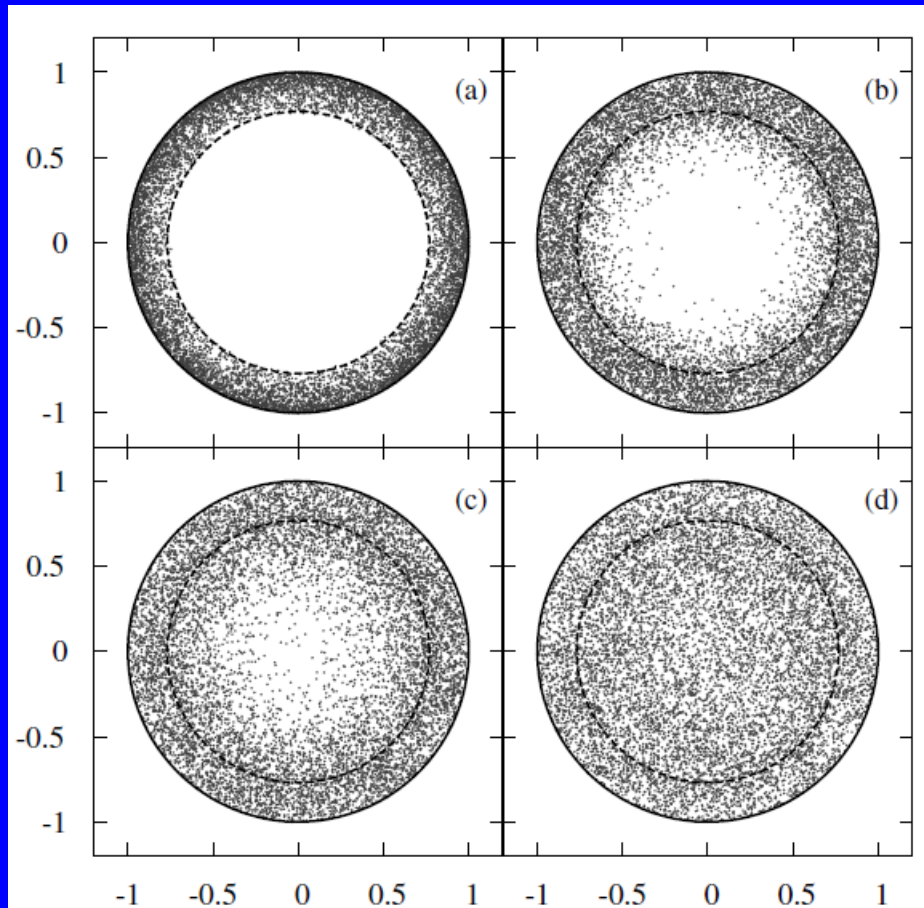
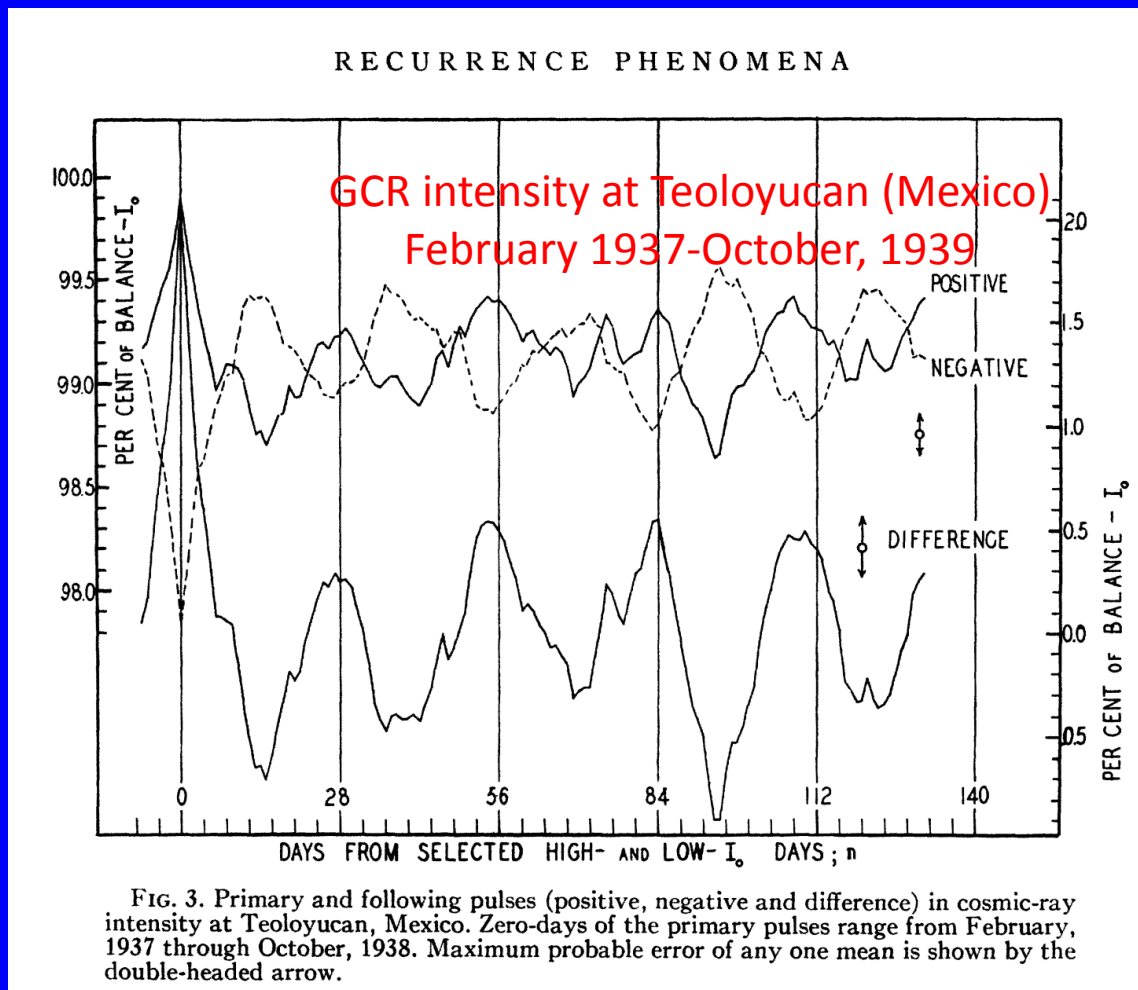


**Figure 8.** Cosmic-ray particle distribution on the  $r - \varphi$  plane for the case that the flux rope is located at 0.1 AU from the Sun and that the cosmic-ray rigidity is 60 GV. Solid and dashed circles show the flux rope edge and the boundary of the forbidden region, respectively. Panels (a)–(d) are for the time  $t = 2.5, 250, 750,$  and  $2500 (\omega_p^{-1})$ .

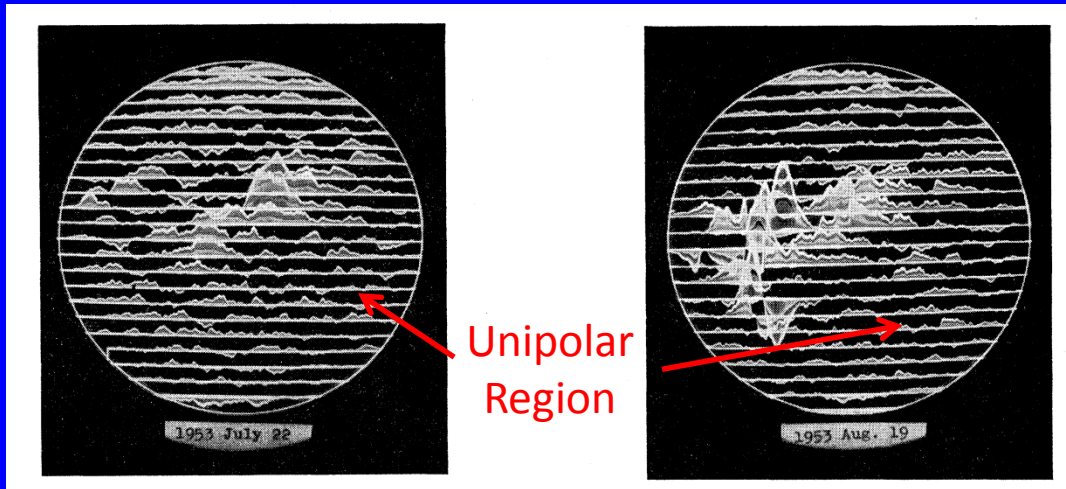
Cosmic rays are scattered into the interior of a flux rope in the presence of small-scale irregularities. Otherwise, penetration is limited to  $\sim 1$  Larmor radius.

# Cosmic Ray Depressions Recurring at the Solar Rotation Period (e.g., Monk and Compton, 1939)



Not associated with solar activity, e.g. active regions. More closely related to “M (mystery)” regions lacking sunspots that correlated with recurrent geomagnetic activity.

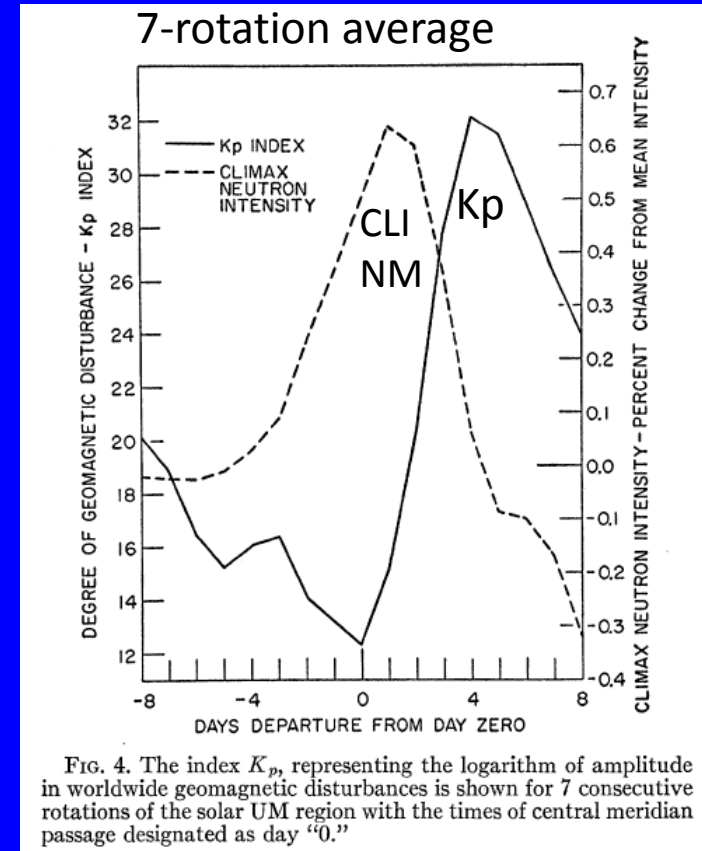
# Simpson, Babcock and Babcock (1955): Association of a “Unipolar” Magnetic Region on the Sun With Changes of Primary Cosmic Ray Intensity



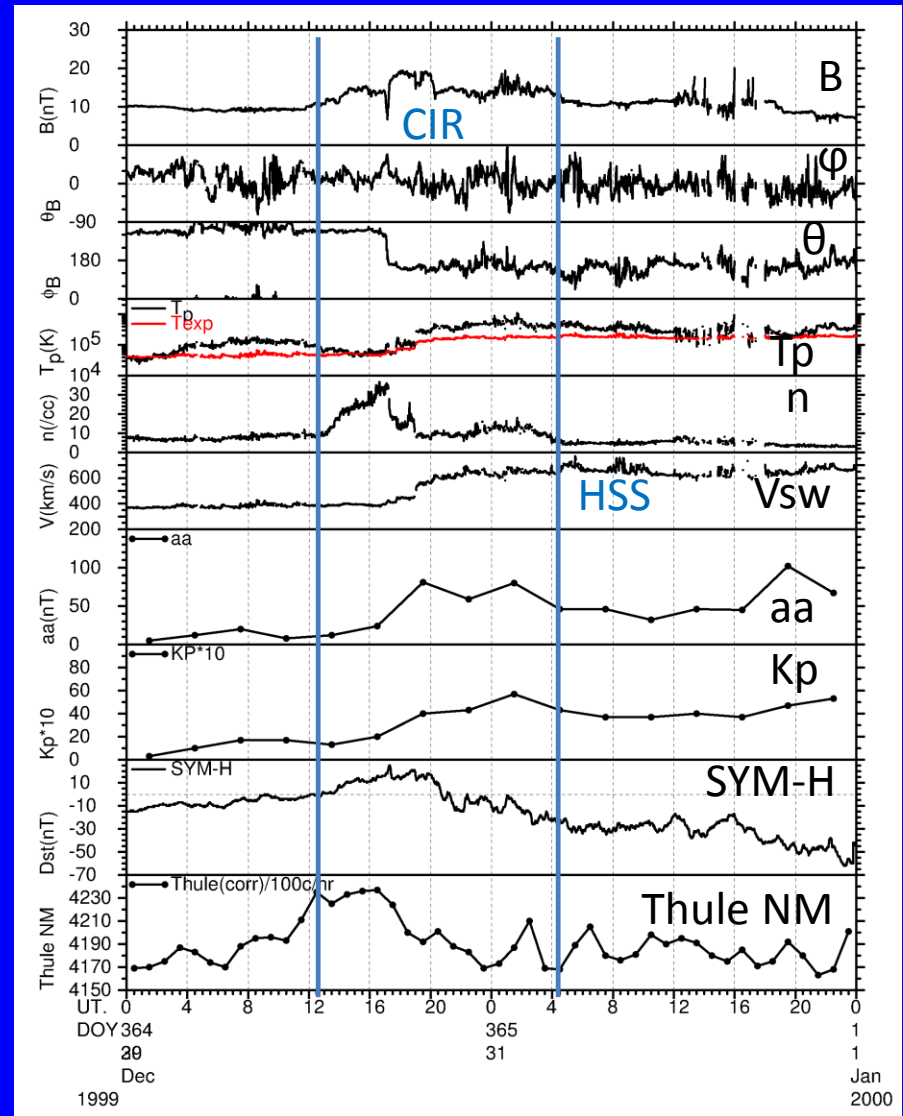
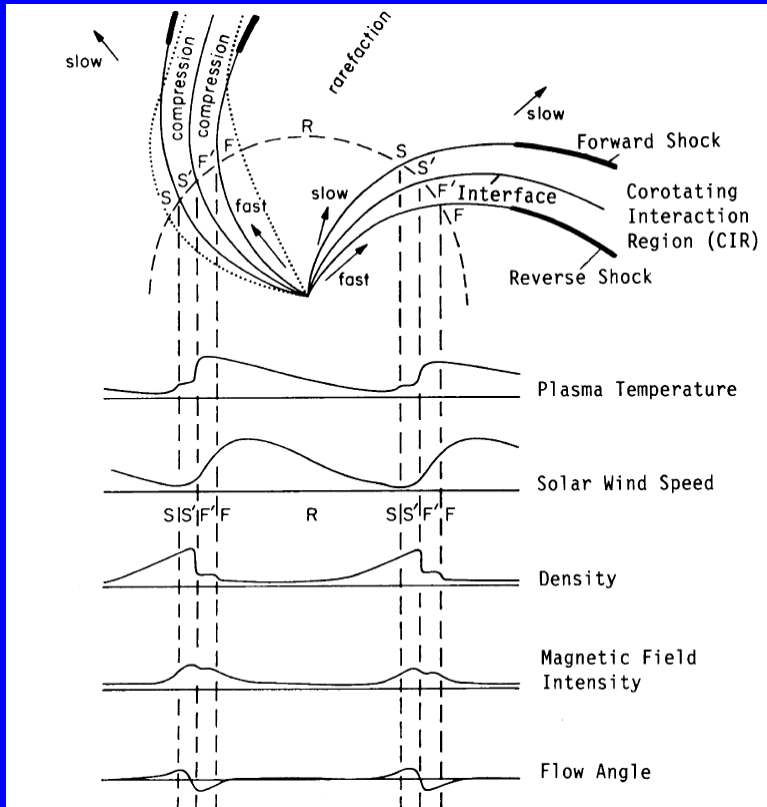
“May have been the first evidence of a coronal hole”  
–Simpson (2000)

GCR intensity tends to peak when UMR is near central meridian, and declines when UMR has rotated to the western hemisphere

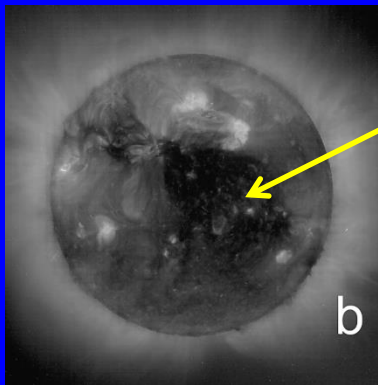
Geomagnetic activity peaks when the UMR is on the western hemisphere and the GCR intensity is declining



# Association of Recurrent FDs with Corotating Interaction Regions/High-speed Streams



Richardson, 2004 after Belcher and Davis, 1971



Coronal hole associated with this high speed stream

SOHO/EIT

Adapted from Richardson, 2004



# Why Use Spacecraft Observations to Study FDs?

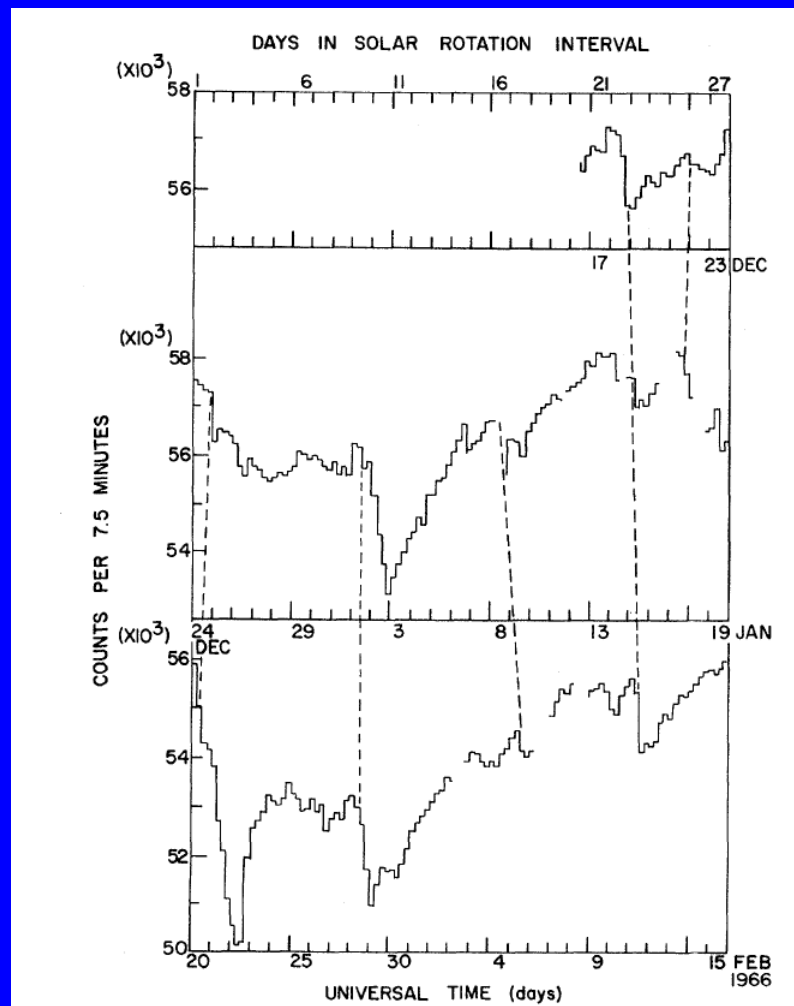
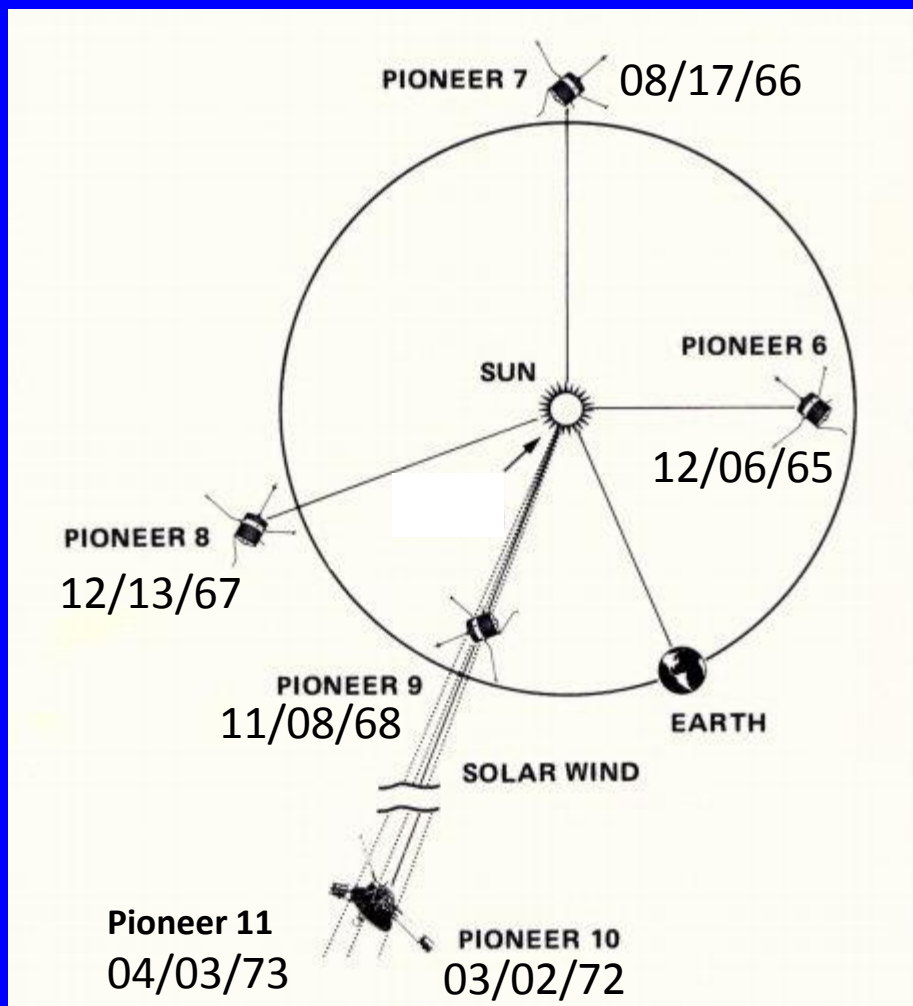
- Multi-point observations of FDs , including far from Earth;
- Intensity variations can be related directly to solar wind structures observed by the same spacecraft;
- No diurnal variation.

## Disadvantages:

- Limited instrument/detector size and weight => restricted energy range, limited counting statistics;
- Telemetry may be limited;
- Relatively expensive;
- Limited mission duration;
- Not many locations, but  $> 1$

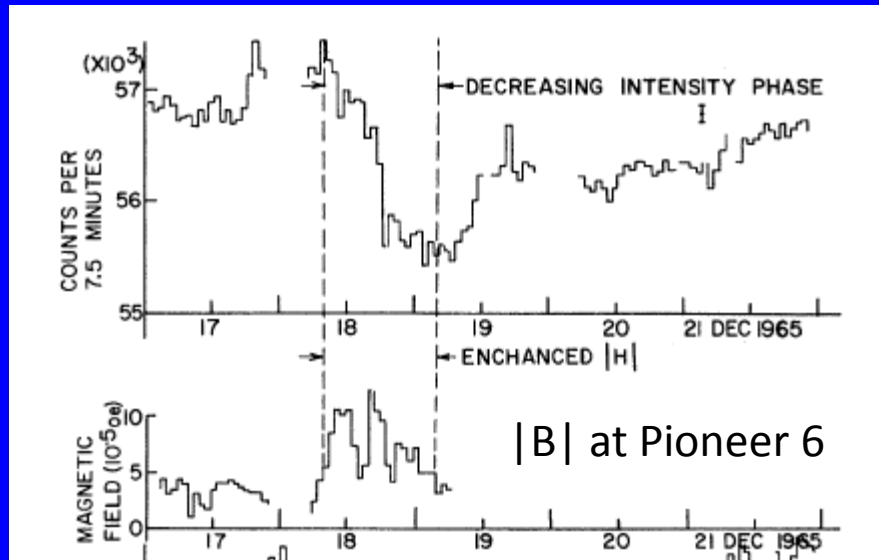
# McCracken, Rao and Bukata, Phys. Rev., 17, 928, 1966. Pioneer 6

## Recurrent FDs (>7.5 MeV) at Pioneer 6

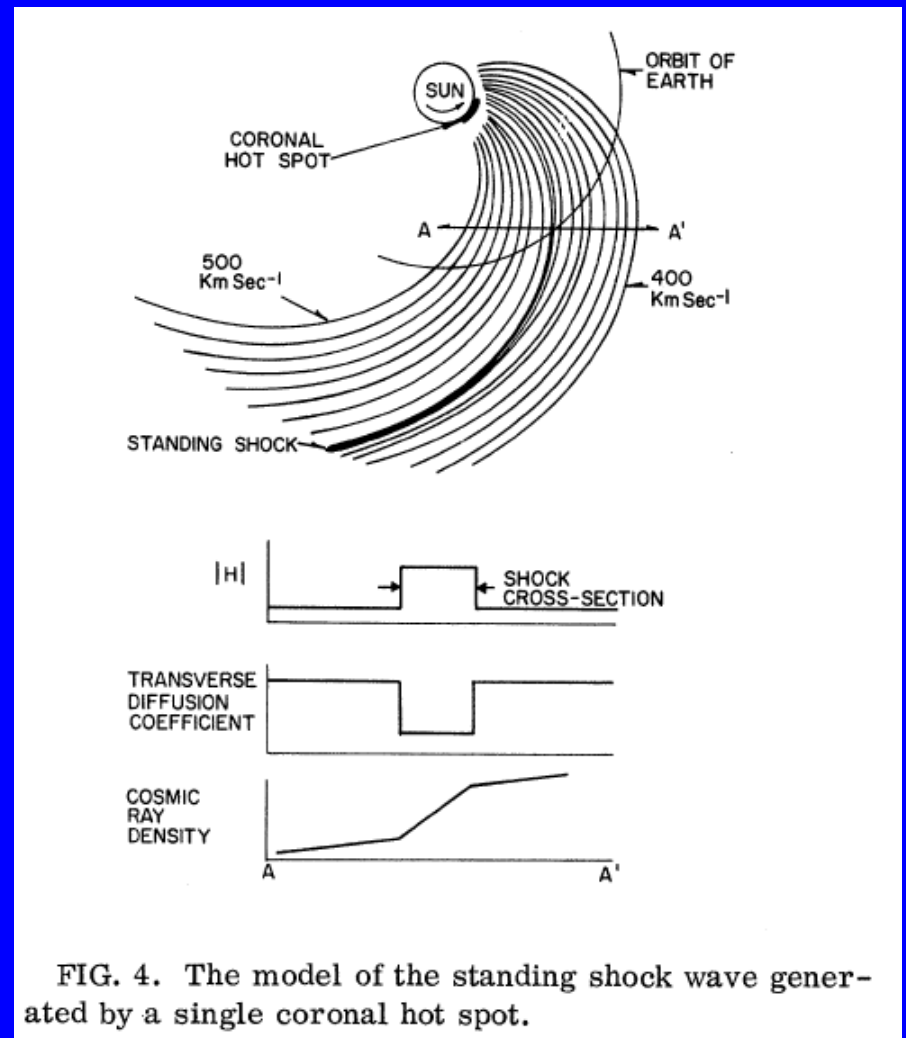


GCRs detected by  $38\text{cm}^2 \times 2.2\text{cm}$  CsI scintillator;  $\sim 56000$  counts/7.5 minutes,  $\sim 0.4\%$  statistical error

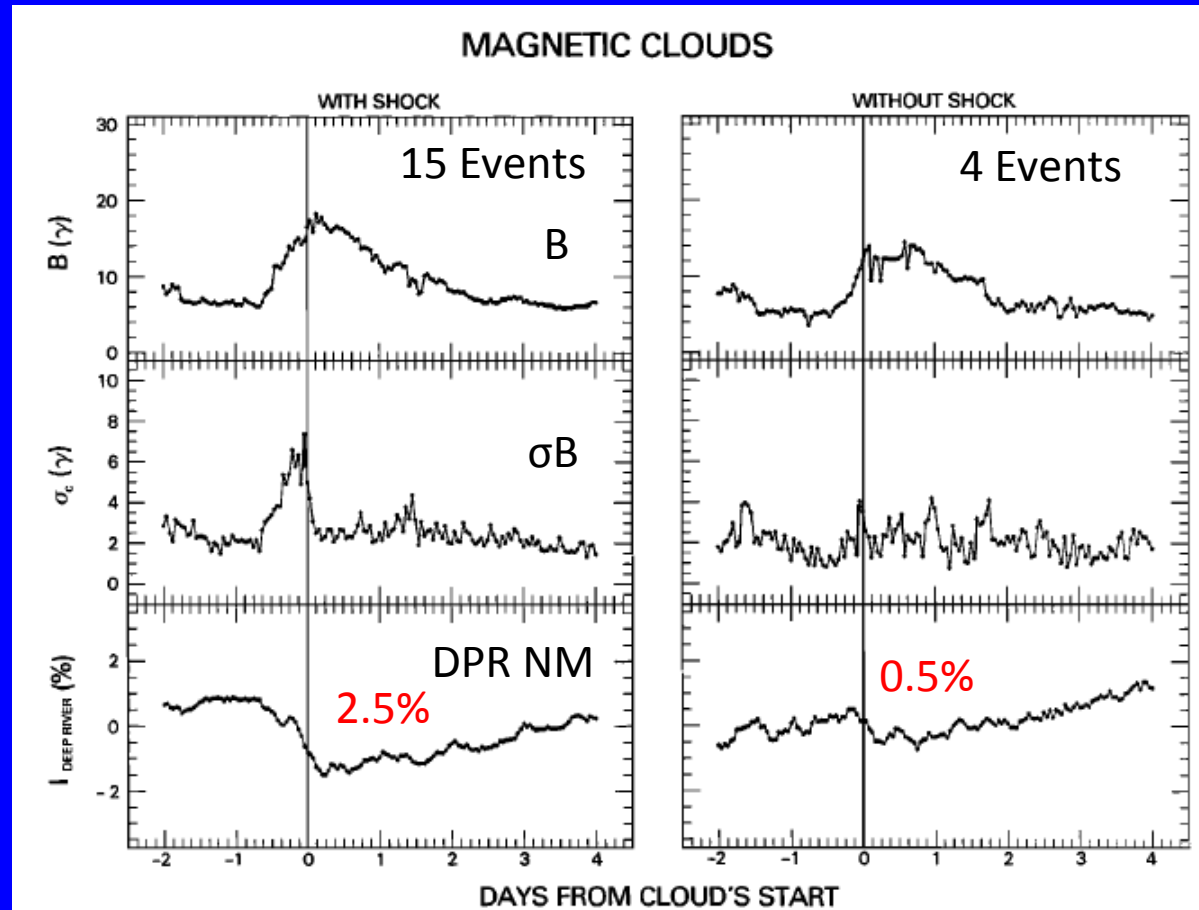
# McCracken, Rao and Bukata (1966) (cont.)



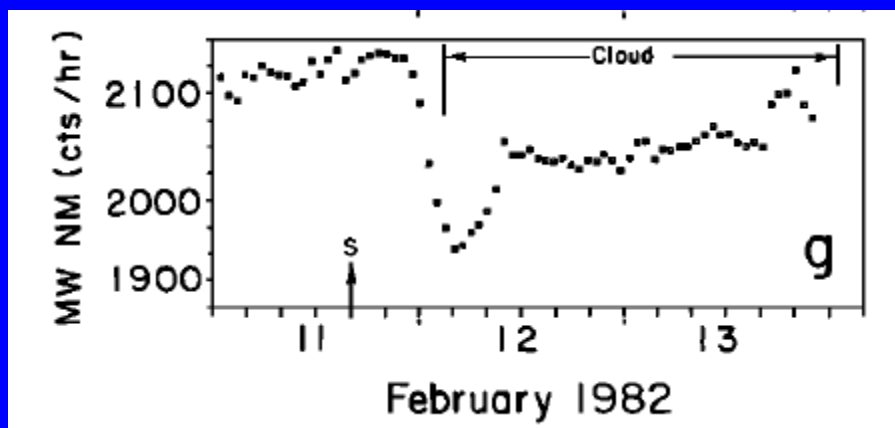
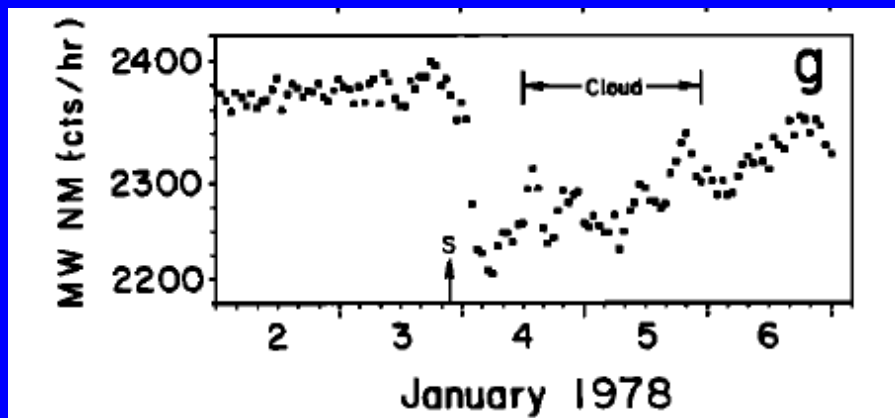
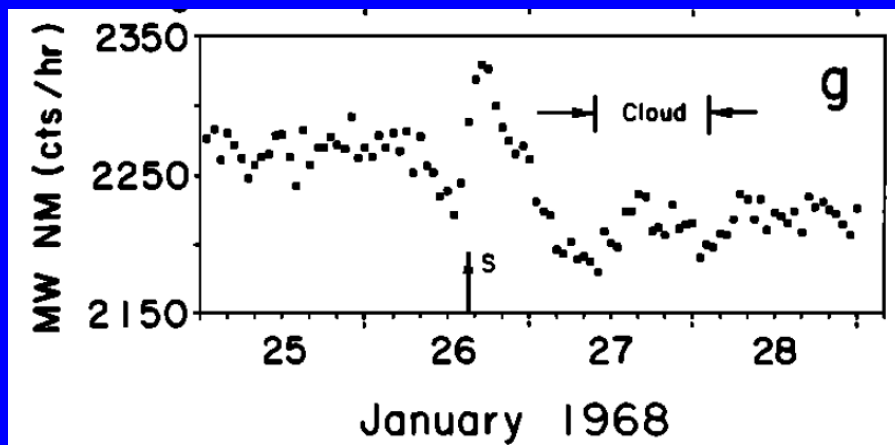
What we would now call a corotating interaction region.



*Zhang and Burlaga, 1988: Superposed Epoch Analysis of Deep River NM Data During the Passage of Magnetic Clouds With or Without Preceding Shocks*



Concluded that FDs are predominantly generated by the shock/sheath; MCS make only a minor contribution.

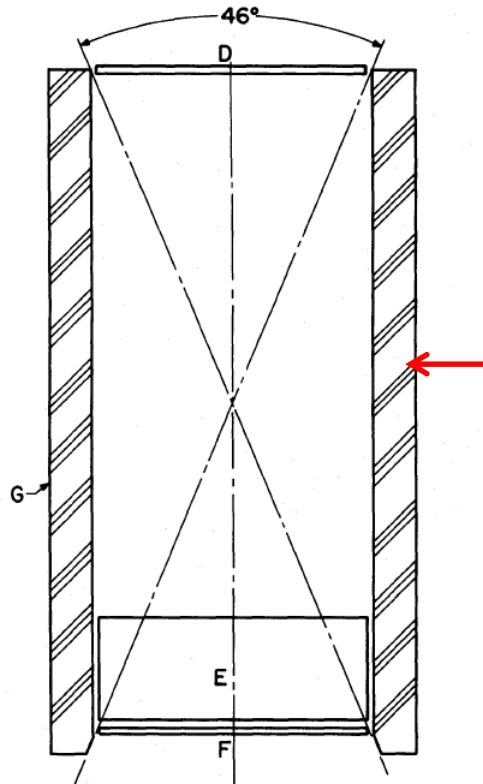


*Lockwood, Webber and Debrunner (1991), Mt. Washington NM*

“the role of magnetic clouds in producing Forbush decreases is relatively unimportant”.

“The major portion of the decrease is produced by reduced particle diffusion in [the turbulent region behind the shock]”.

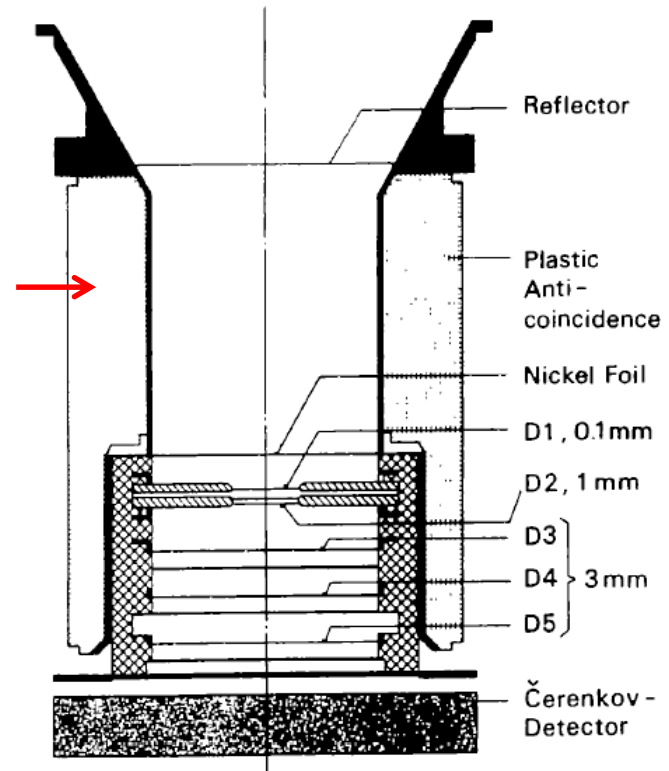
# IMP 8 Goddard Medium Energy Detector Telescope



D, F - 1MM x 20 CM<sup>2</sup>  
CsI SCINTILLATOR  
E - 2 CM x 20 CM<sup>2</sup>  
CsI SCINTILLATOR  
G - PLASTIC SCINTILLATOR

Anti-coincidence guard (Plastic Scintillator)

# Helios 1/2 E6 Instrument (U. of Kiel)



Reflector

Plastic Anti-coincidence

Nickel Foil

D1, 0.1mm

D2, 1mm

D3 } 3mm

D4 }

D5 }

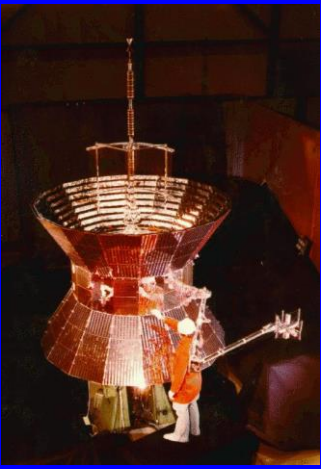
Čerenkov-Detector

## Why use anticoincidence guards?

- Large detection volume - orders of magnitude higher counting rates than particle telescopes;
- Lower rigidity range than NMs => greater % modulation.

However,

- Not intended for science!
- Energy response and viewing geometry are poorly/un-defined;
- Calibration is not checked and long-term drifts in response may occur - provide a qualitative view of GCRs;
- Count rates well below those of NMs.
- Detect (and often dominated by) solar particles above ~60 MeV
- Receive distain from Frank McDonald!



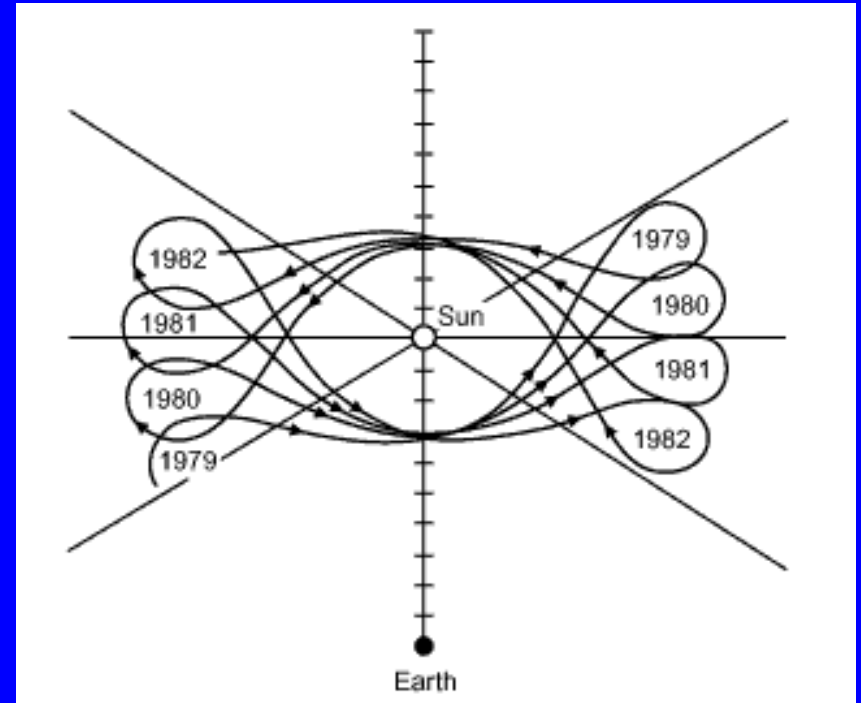
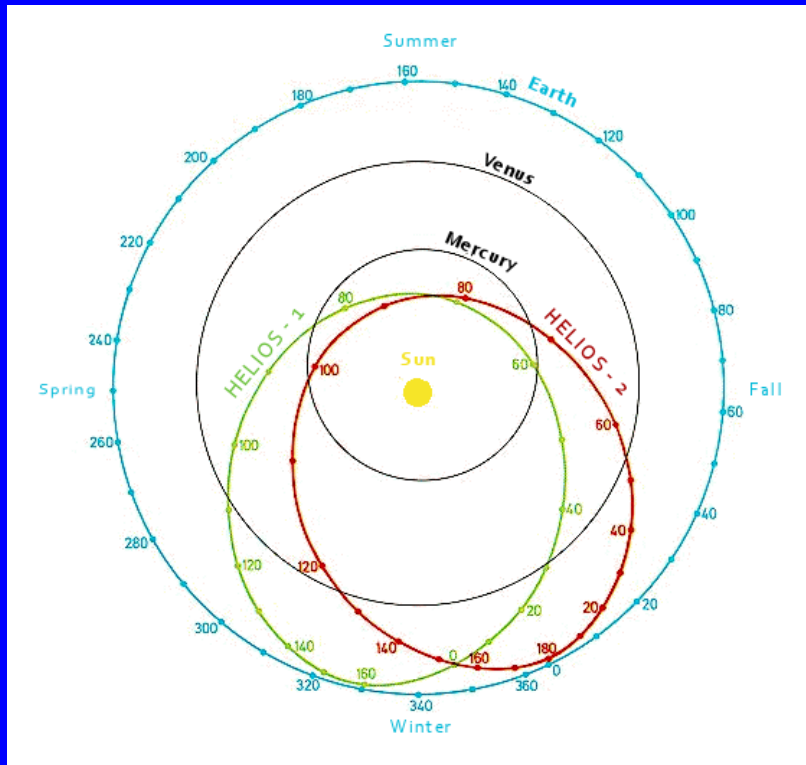
# Helios Spacecraft Orbit (0.3-1 AU)

Helios 1 Launch: 10 December, 1974

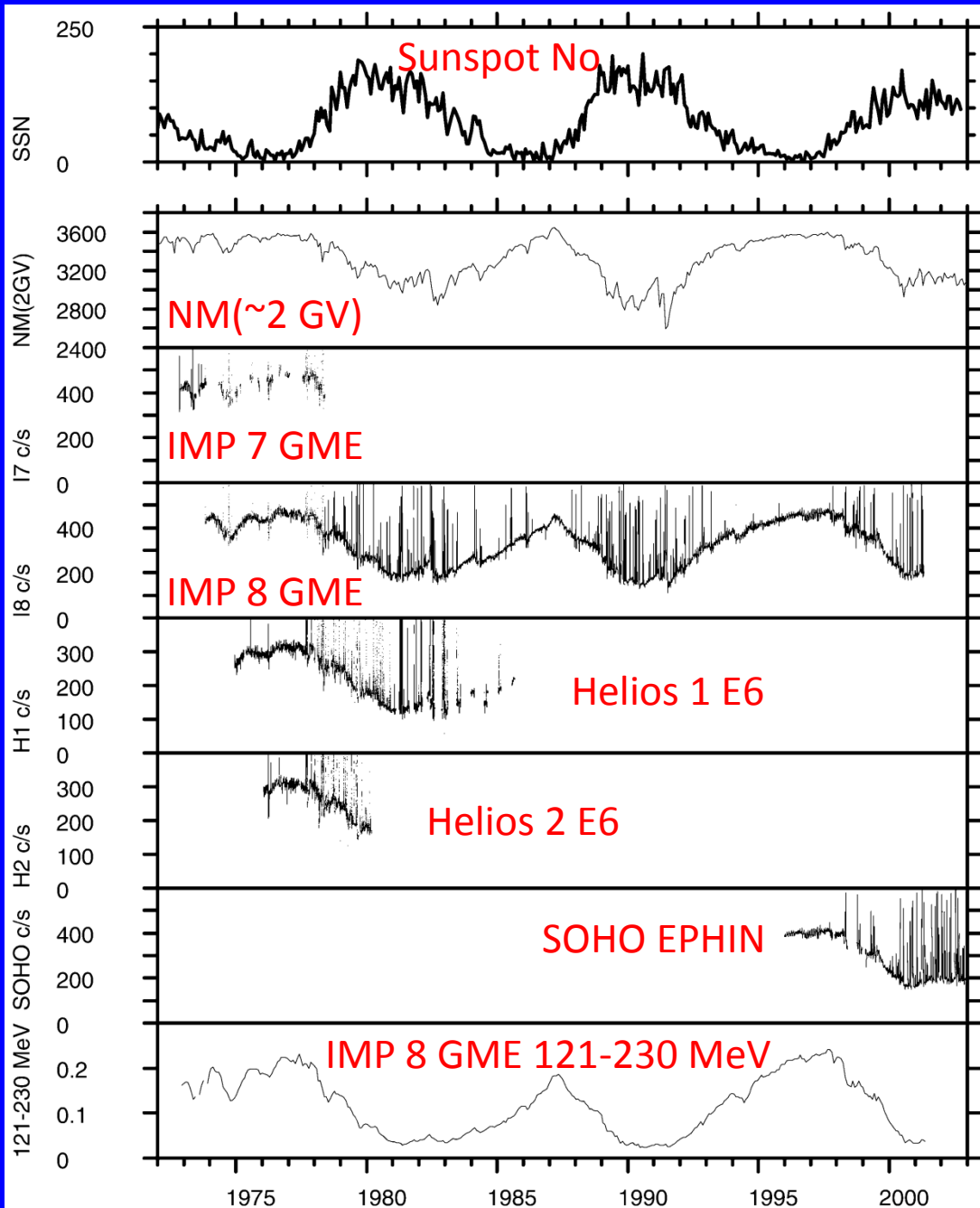
Helios 2 Launch: 15 January, 1976

Fastest spacecraft ( $\sim 70$  km/s at perihelion), until Juno, Solar Probe Plus

Helios 1 orbit relative to the Earth-Sun line in 1979-1982







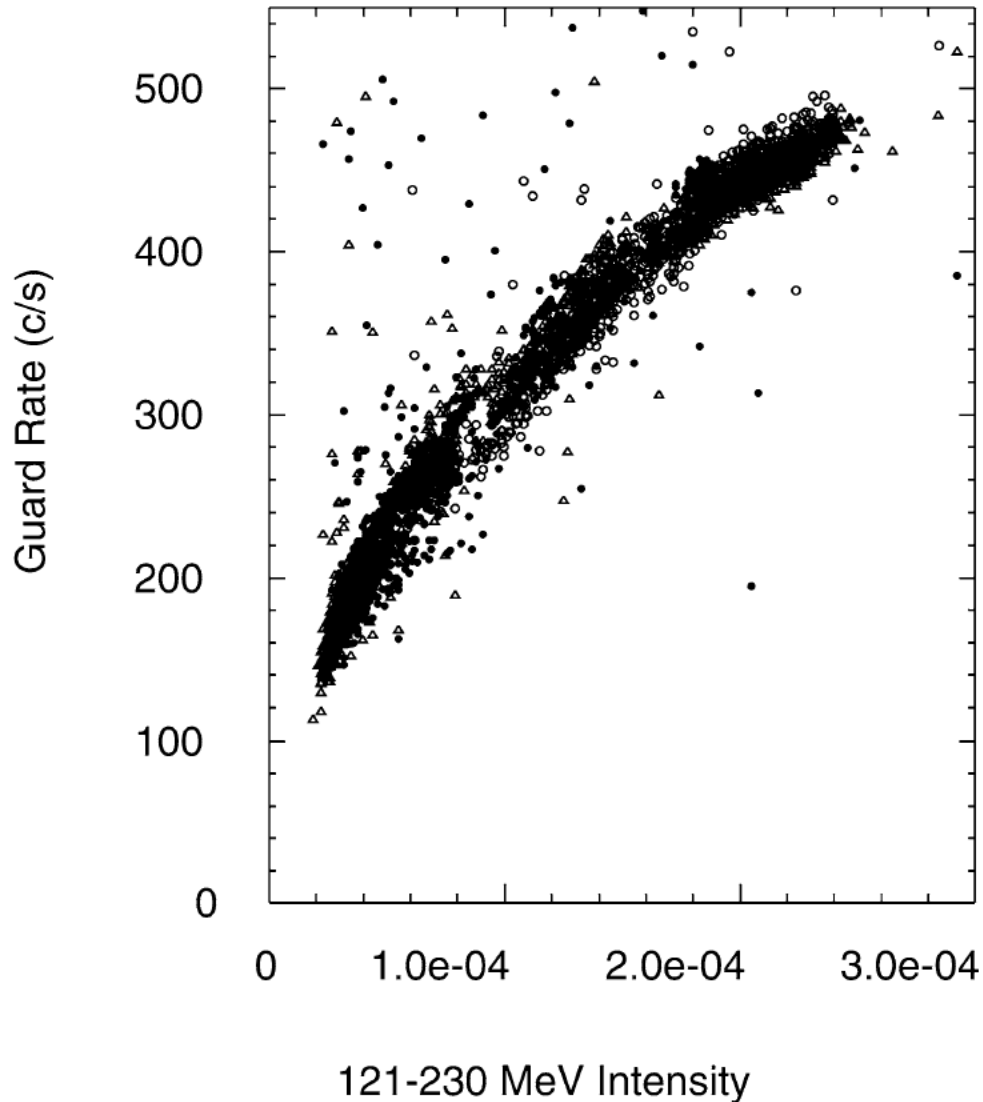
## Examples of Anticoincidence Guard Count Rates in 1972-2002

Long-term solar cycle modulation of GCRs is evident, with brief FDs.

Upward spikes are solar particle events (removed in IMP 8 121-230 MeV intensity)

*Richardson, 2004*

# Long-term Stability of the IMP 8 GME Guard Counting Rate Over 25 Years of Observations (1973-1998; 2 day averages)



The 121-230 MeV IMP 8 channel was carefully re-calibrated during the mission to provide a baseline for Voyager in the outer heliosphere.

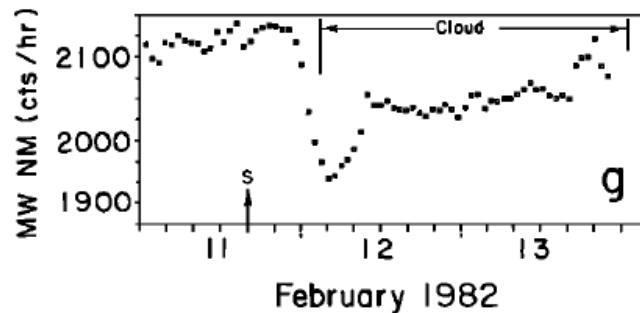
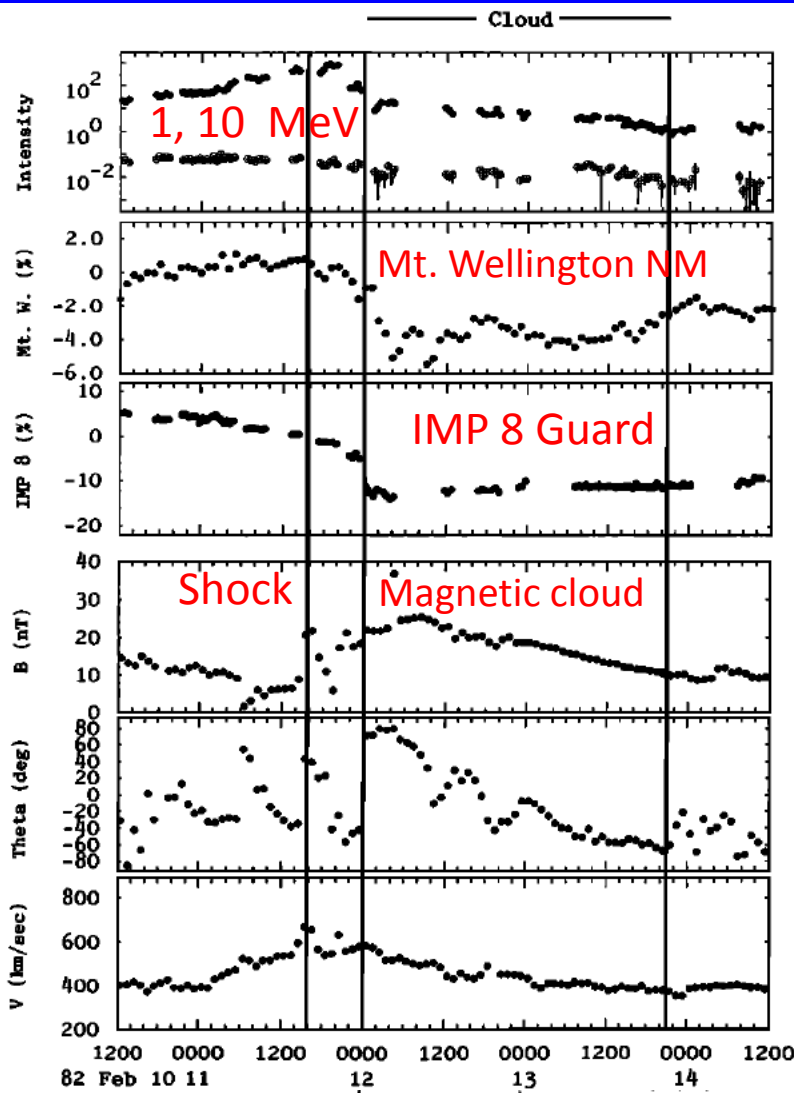
The consistency of the guard rate vs. 121-230 MeV track indicates the remarkable stability of the guard rate even though no corrections were made and long-term changes e.g. in photomultiplier tube efficiency would have been expected.

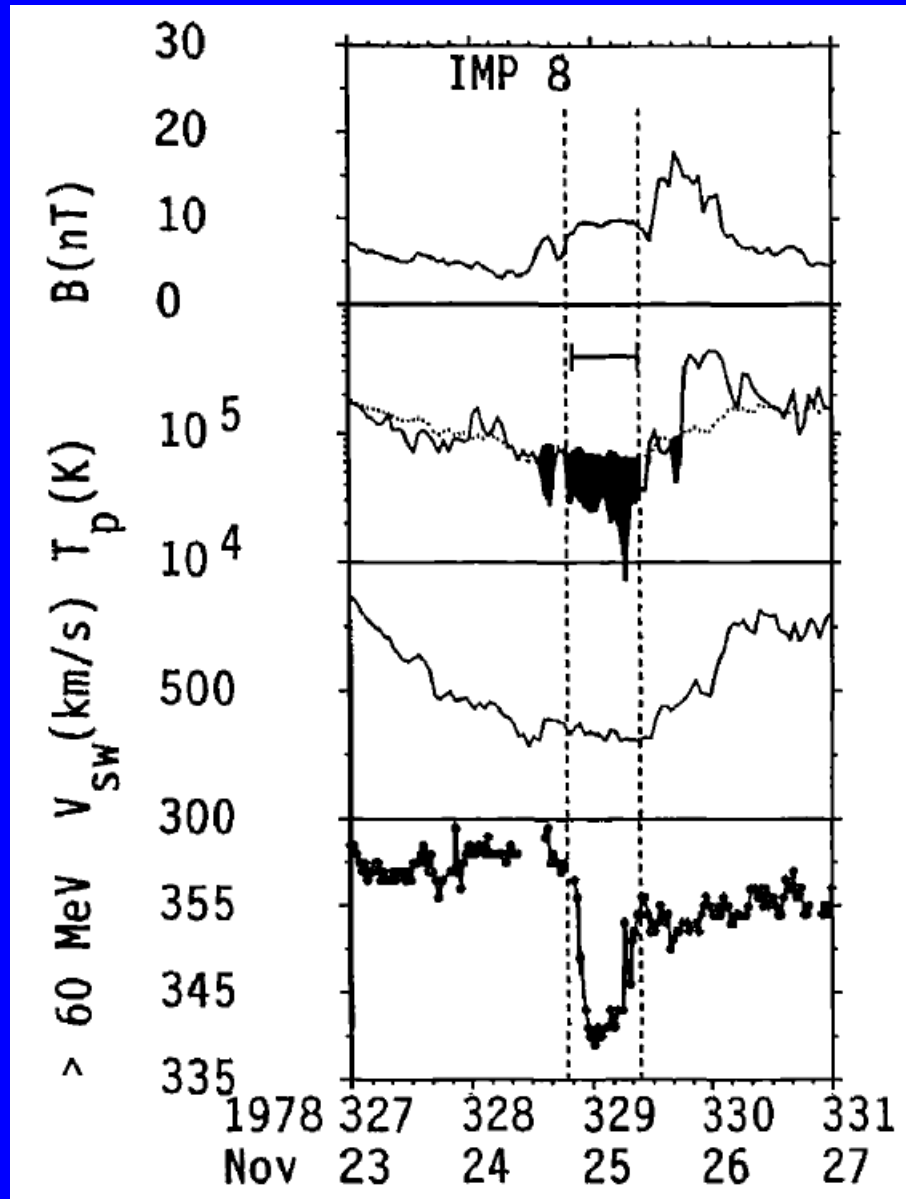
*Richardson, 2004*

# Cane, 1993: "Cosmic Ray Decreases and Magnetic Clouds"

Do magnetic clouds contribute to FDs?

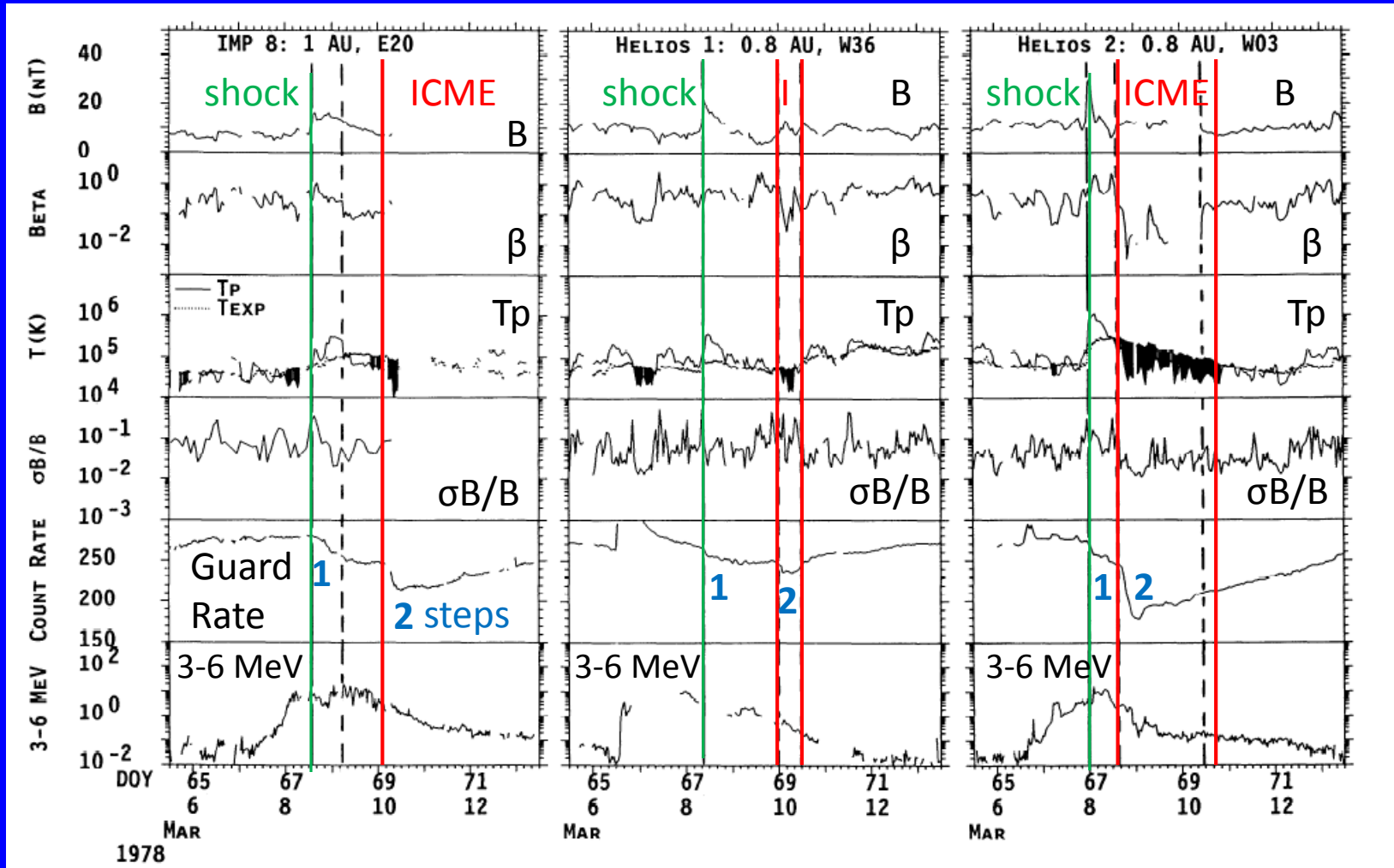
- Sheath only : *Badrudin et al. 1985, 1991; Zhang and Burlaga 1988; Lockwood, Webber, and Debrunner 1991.*
- MC contributes (cf. two step FDs): *Barnden, 1973; Barouch and Burlaga, 1975; Sanderson et al., 1990.*
- IMP 8 guard rate clearly shows GCR decreases on entry to the magnetic clouds of *Zhang and Burlaga 1988.*





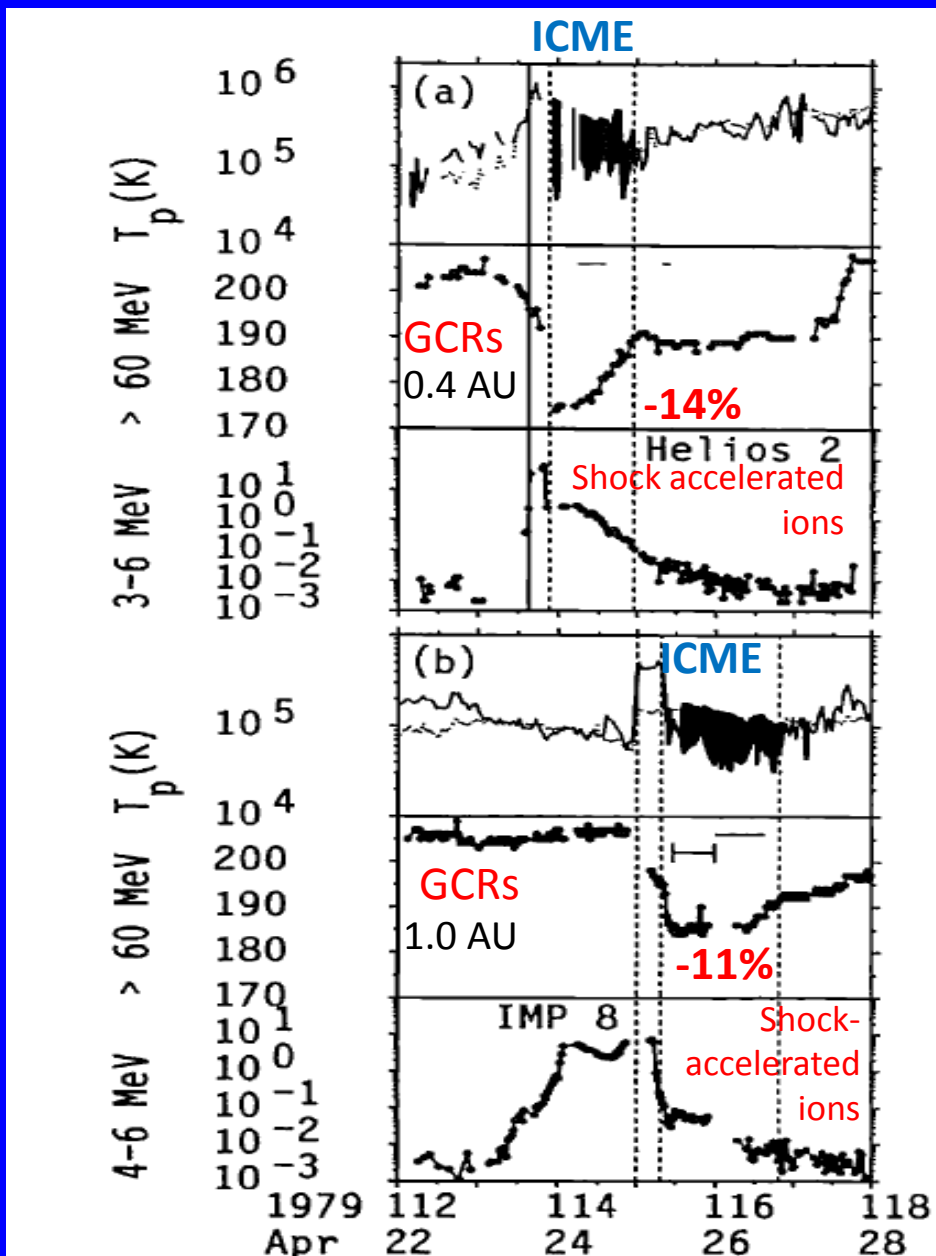
Example of a brief GCR decrease during passage of a small magnetic cloud in November 1978 observed by the IMP 8 GME guard.

# Observations of the Same Shock and ICME at Helios 1, 2 and IMP 8



Largest FD, strongest shock and most extended ICME interval seen at S/C closest to solar event location.

Location of the GCR second step moves relative to the shock and is consistent with entry into the ICME. (Cane, Richardson, von Rosenvinge, Wibberenz, JGR, 1994)

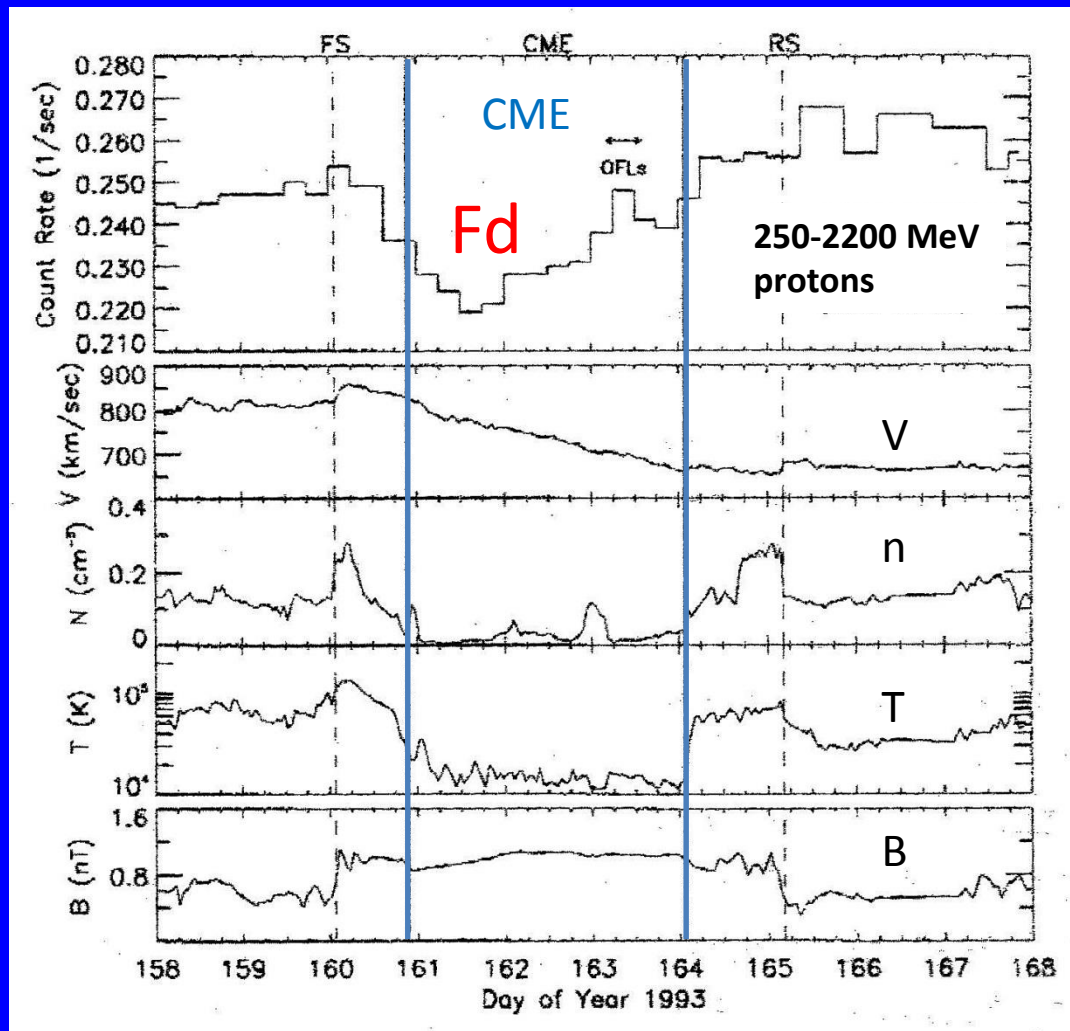


An FD Observed at 0.4 AU by Helios 2 and by IMP 8 at 1 AU When Separated by  $5^\circ$  in Longitude

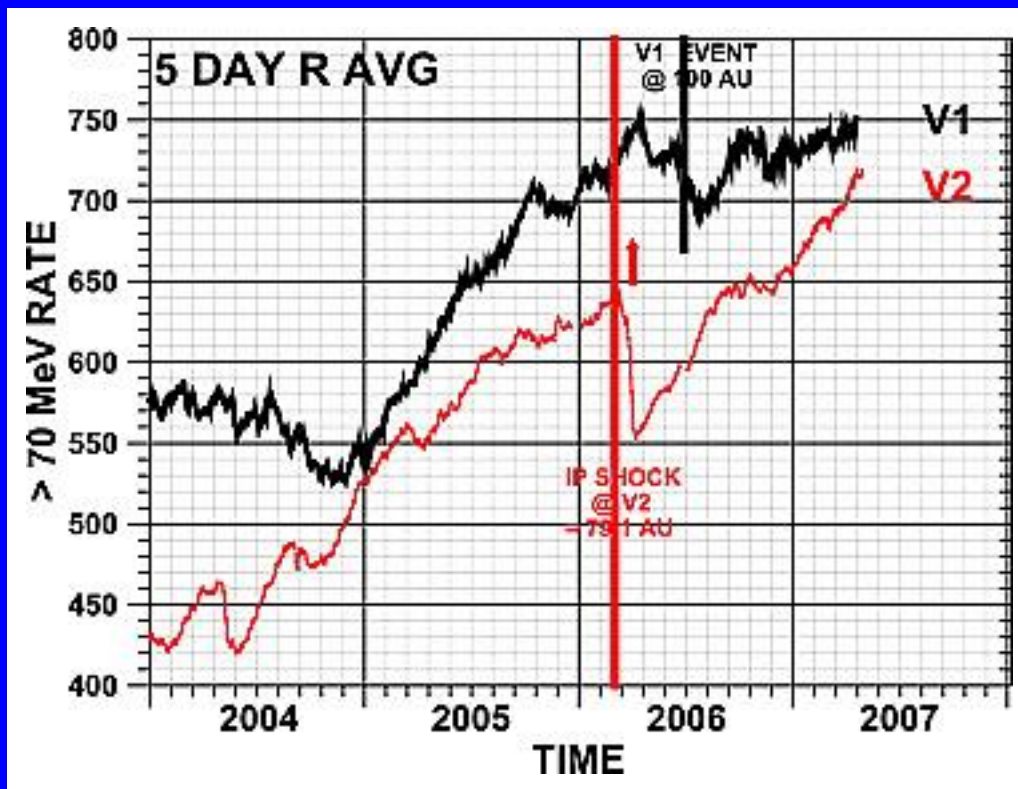
The total GCR (guard rate) decrease is 14% at 0.4 AU and 11% at IMP 8, consistent with GCRs filling in the intensity depression further from the Sun.

On entry to the ICME, there is a  $\sim 90\%$  drop in the  $\sim 5$  MeV shock-accelerated particle population in each case.

# An ICME-Associated Forbush Decrease Observed by Ulysses at 33°S, 4.6 AU (*Bothmer et al., 1997*)



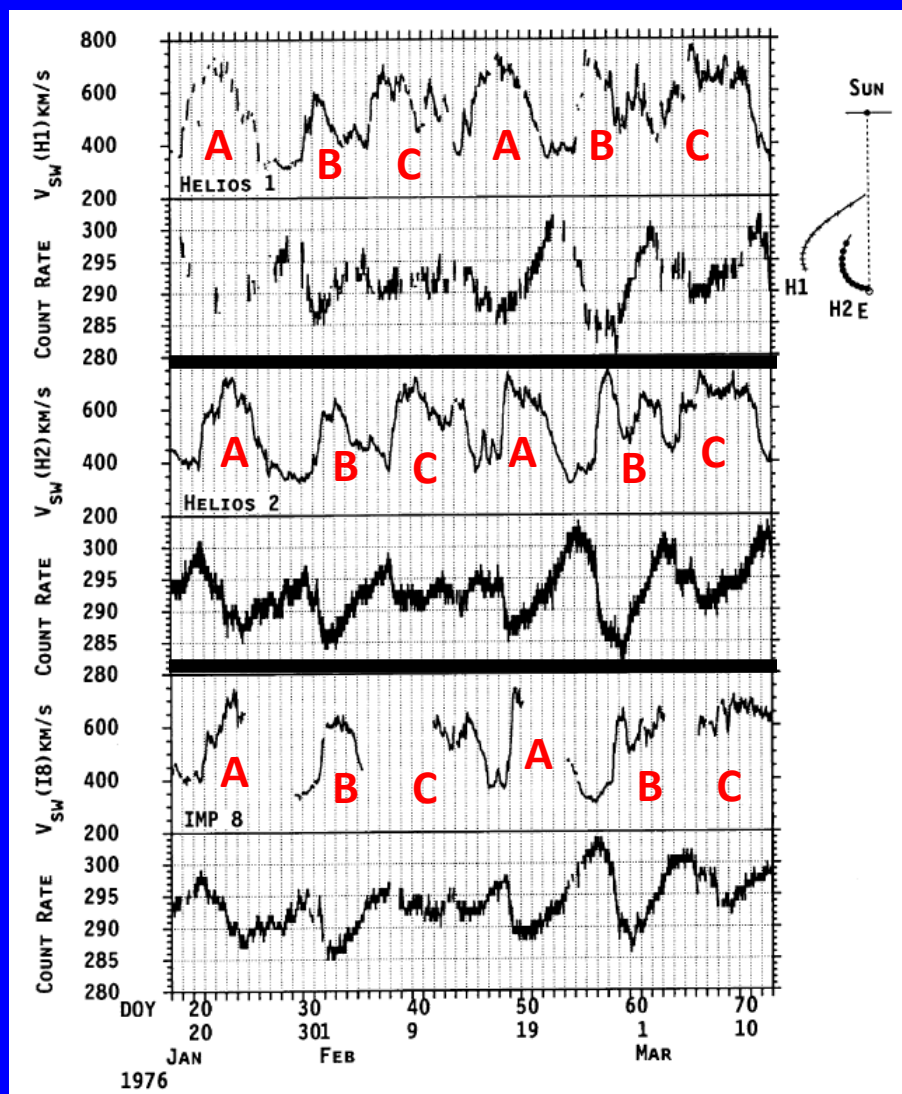
# Forbush Decreases at Voyagers 1 (100 AU) and 2 (79 AU) (Webber et al., 2007)



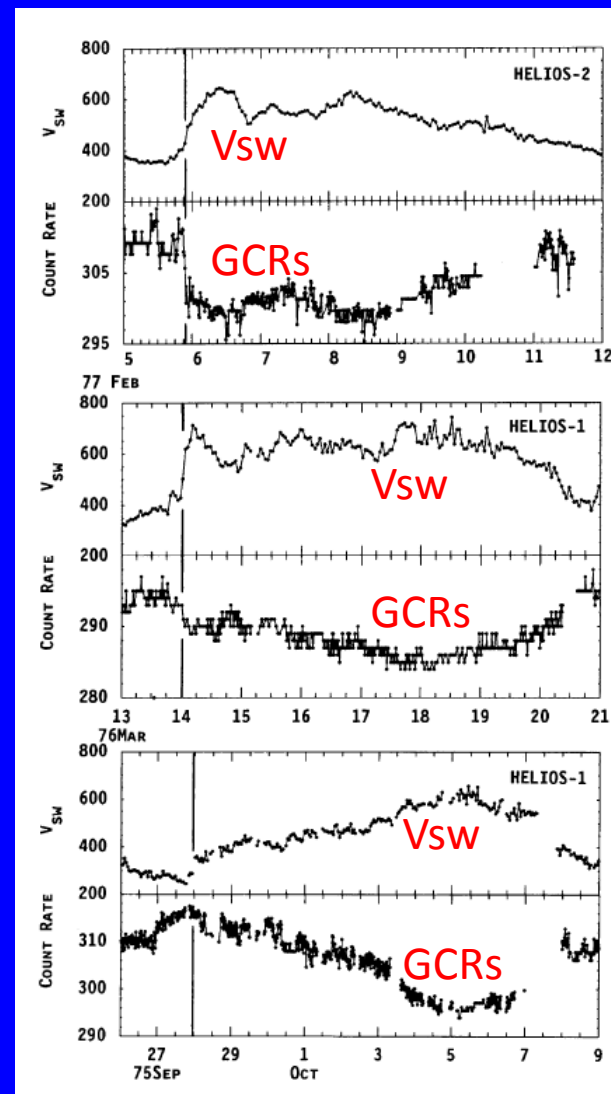


# Recurrent Decreases: Anti-correlation between GCR Intensity and Solar Wind Speed

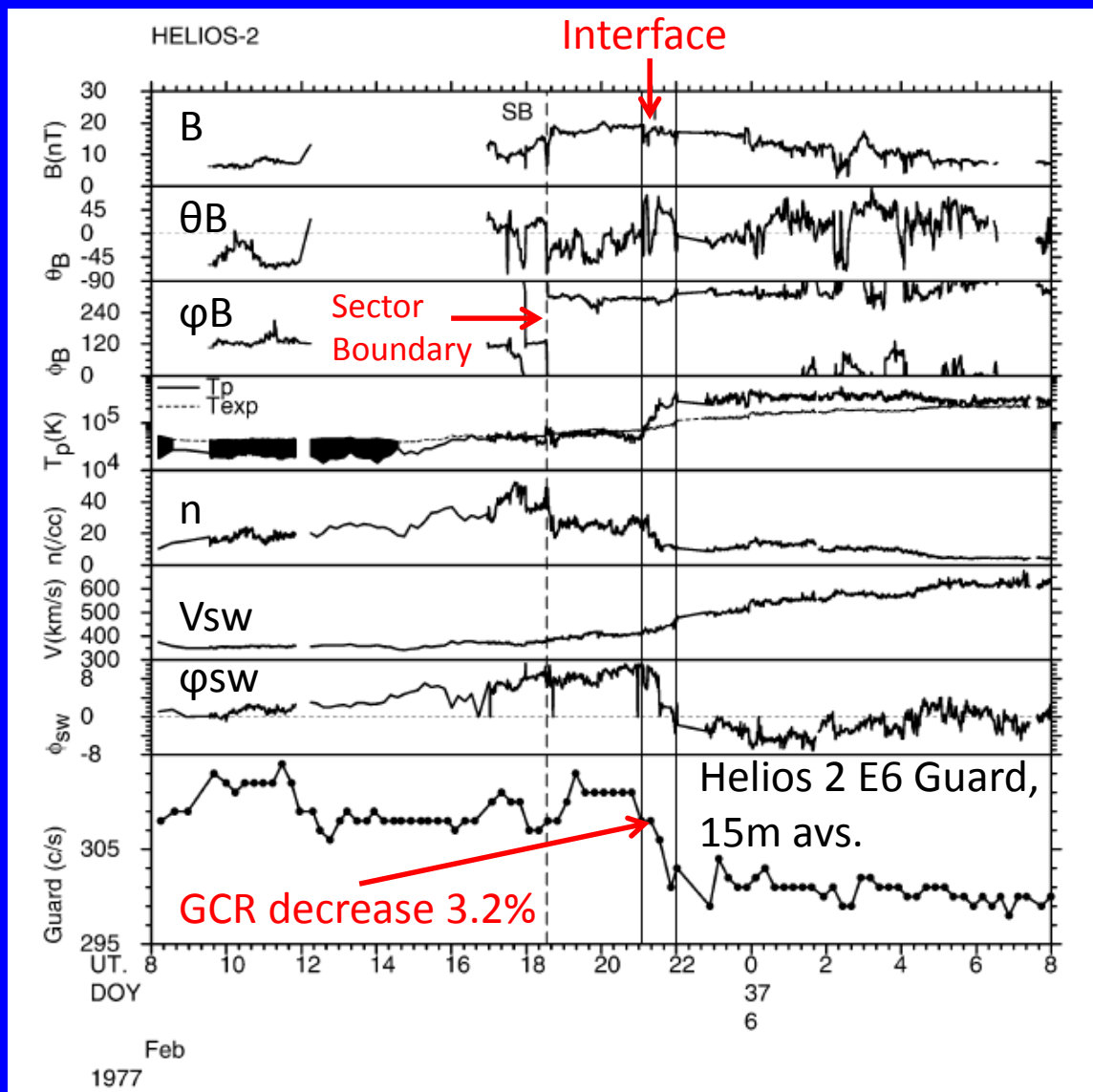
## 3 streams corotating past Helios 1, 2 and IMP 8



## 3 individual streams at Helios



# Corotating GCR Decreases Typically Commence at the Stream Interface Inside the CIR (Helios 2)



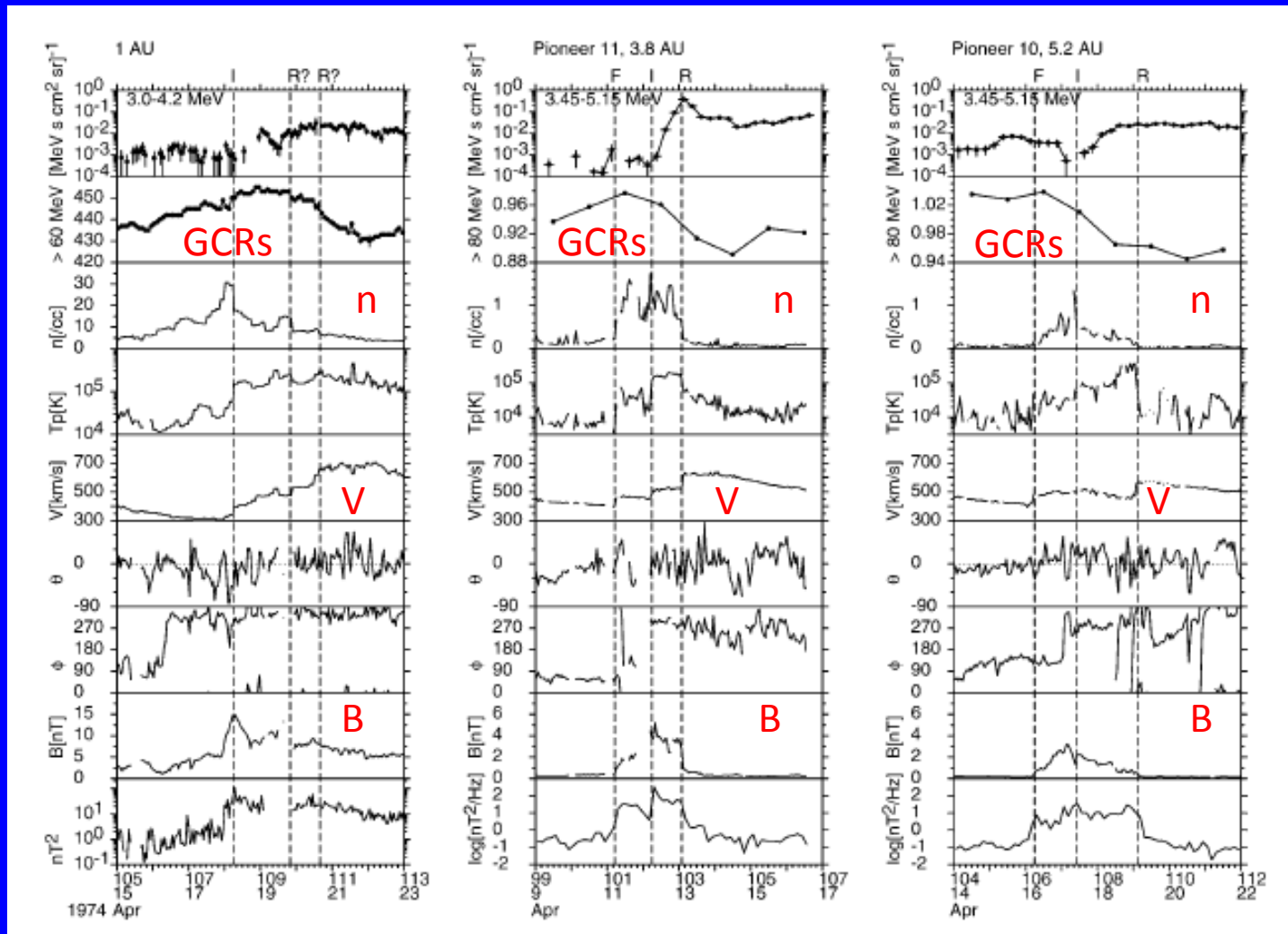
Stream interface - separates slow (denser, cooler) and fast stream (less dense, hotter) plasma within the CIR.

Characterized by increases in solar wind speed, proton temperature, decrease in density, west to east solar wind flow inflection.

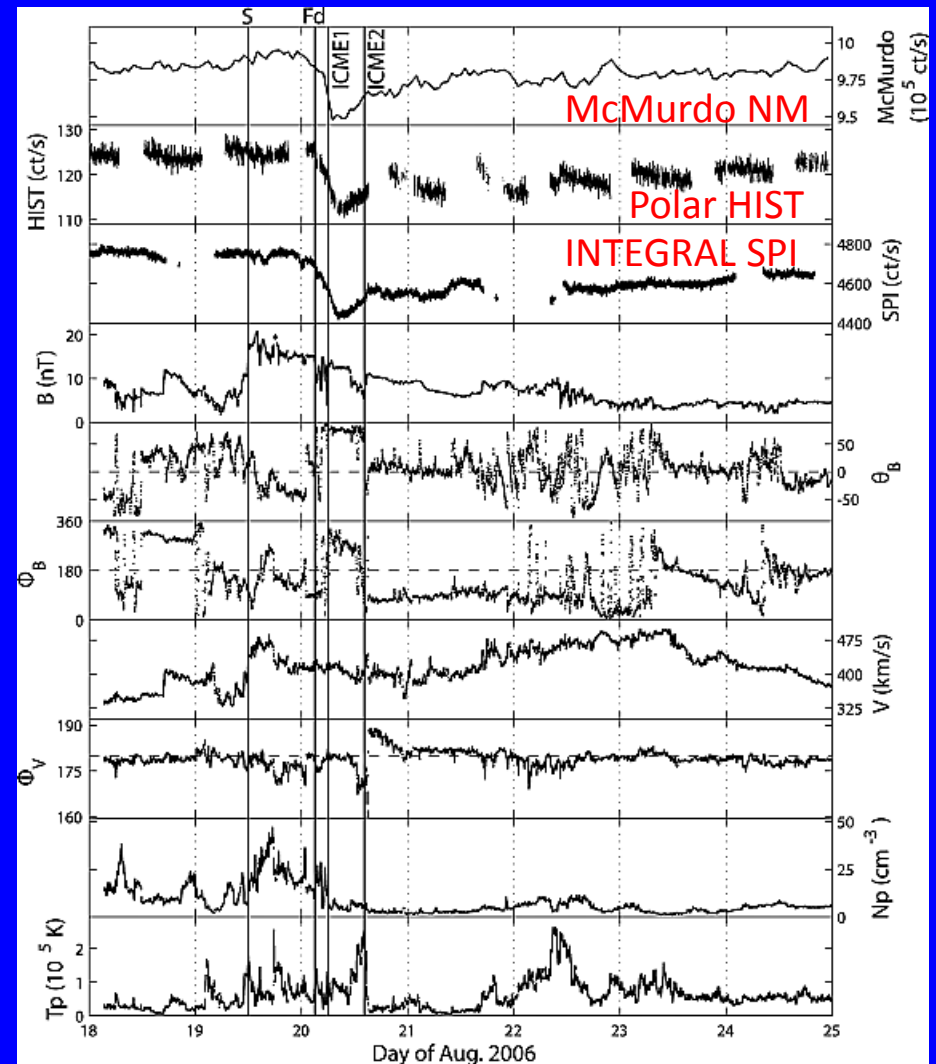
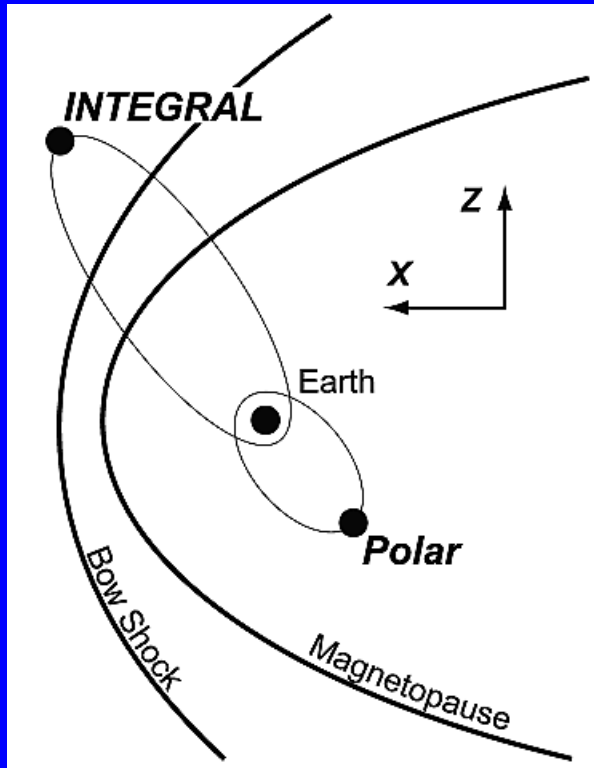
The GCR intensity typically drops abruptly in the vicinity of the interface, as in this example.

GCR decreases are not associated consistently with the CIR-associated B increase or sector boundary/current sheet crossing.

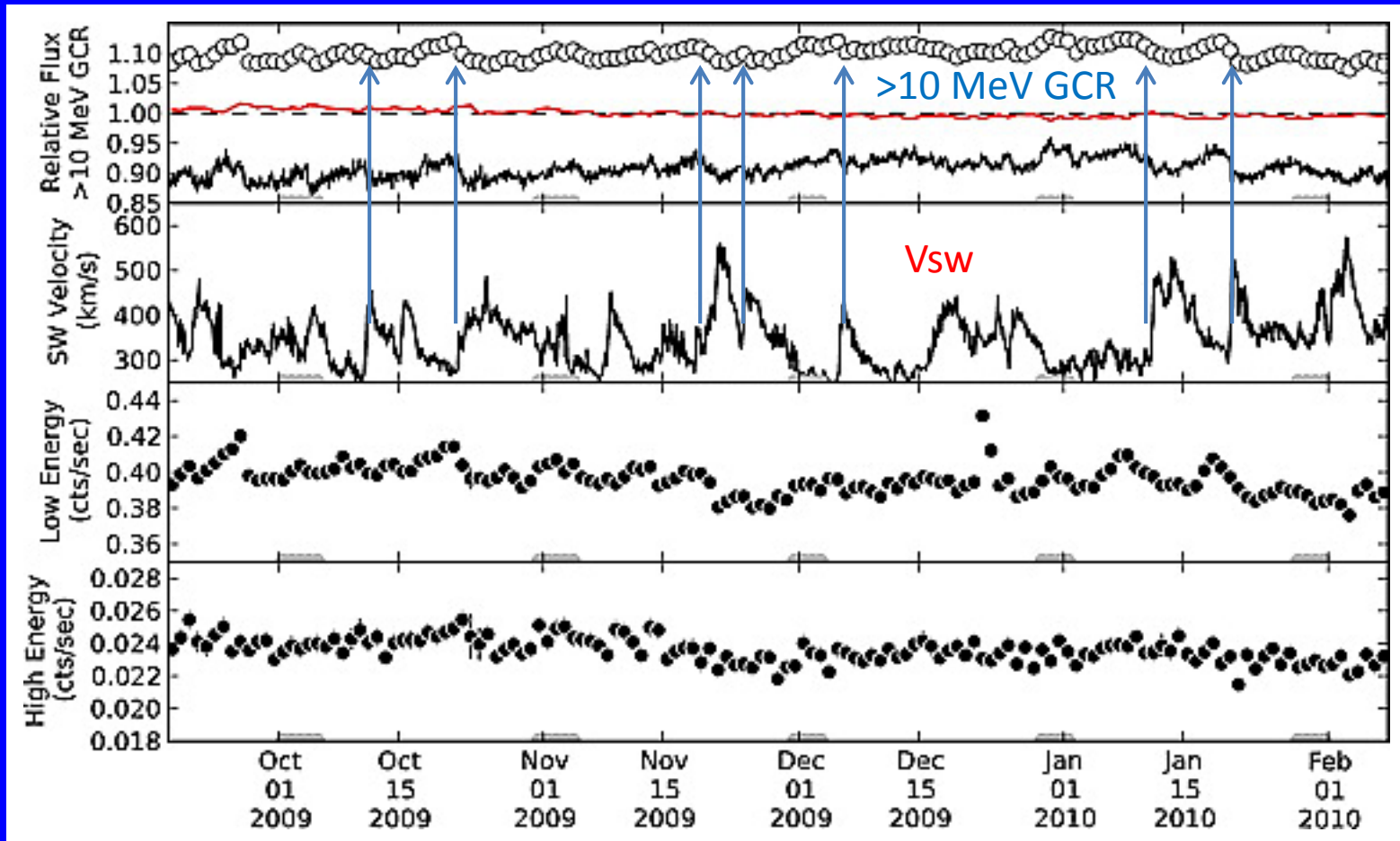
# A GCR decrease associated with a CIR observed at 1 AU (IMP 8), 3.8 AU (Pioneer 11) and 5.2 AU (Pioneer 10)



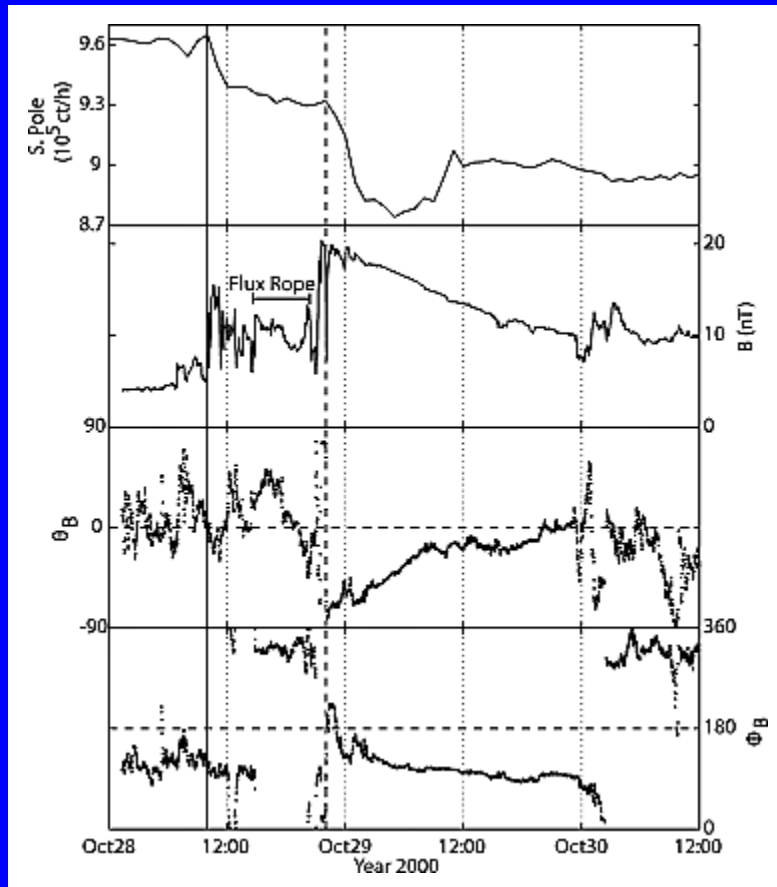
# GCR observations of FDs From Polar HIST Anti-coincidence guard and INTEGRAL SPI (Jordan et al., 2009)



# GCR access to the Moon as measured by the CRaTER instrument on LRO (*Case et al., 2010*)



# “Revisiting Two-step Forbush Decreases” (*Jordan et al., 2011*)



Not a constant decline after shock => not consistent with diffusion in sheath as in the “traditional model”; also flux rope present in sheath.

“We test the traditional model (sic) describing the formation of FDs in GCR intensity.

The model states that if an ICME and its shock encounter a GCR detector, that detector will record a two-step FD.

If only a shock or only an ICME encounter the detector, it will record a one-step FD.”

Conclusion:

“The traditional one- or two-step classification of FDs is inadequate to explain our study.

Each FD must be studied as a unique event in the detailed context of its driving interplanetary conditions.

Only this method will lead to a truly causal classification scheme.”

# GCR Response During the Passage of >300 ICMEs (Richardson and Cane, 2011)

Used data from

- IMP 8 GME Guard.
- Thule NM

80% of ICMEs showed a decrease in GCR intensity

10% - no decrease

10% - increase

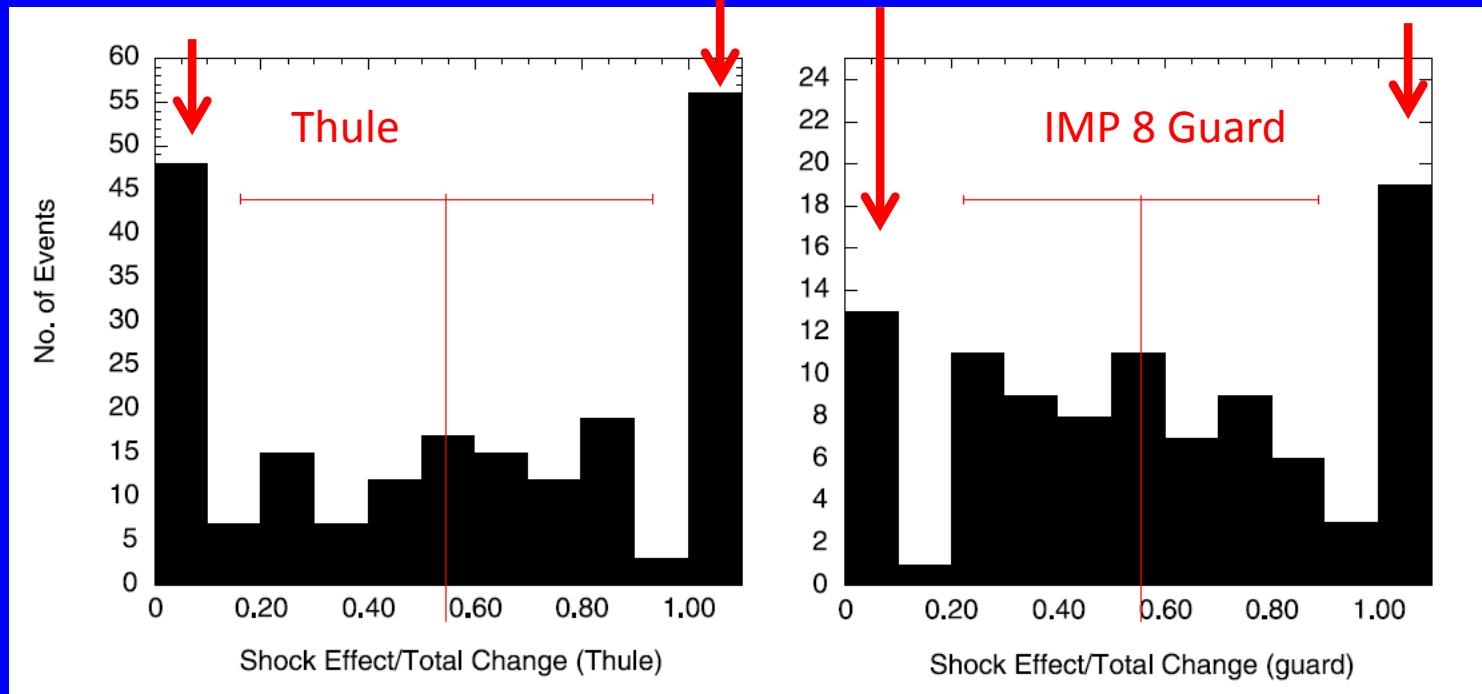
# Contributions of the First Step (Shock Effect) and Second Step (ICME) to the Total GCR Decrease are Variable

No 1<sup>st</sup> step

No 2<sup>nd</sup> step

No 1<sup>st</sup> step

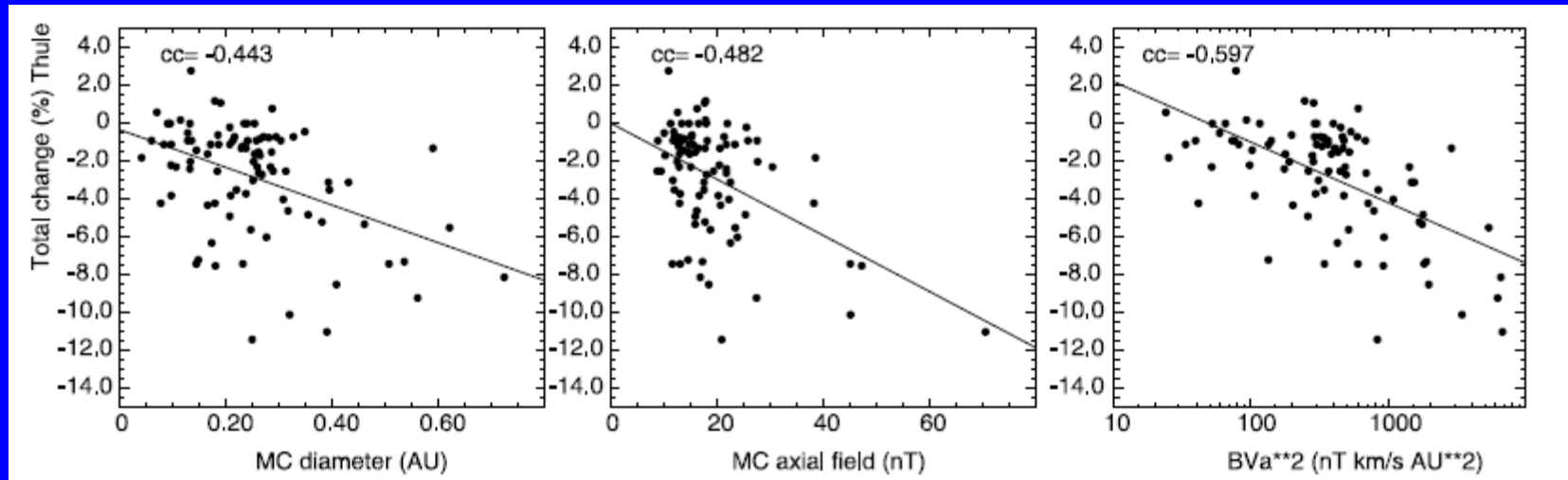
No 2<sup>nd</sup> step



*Richardson and Cane, 2011*



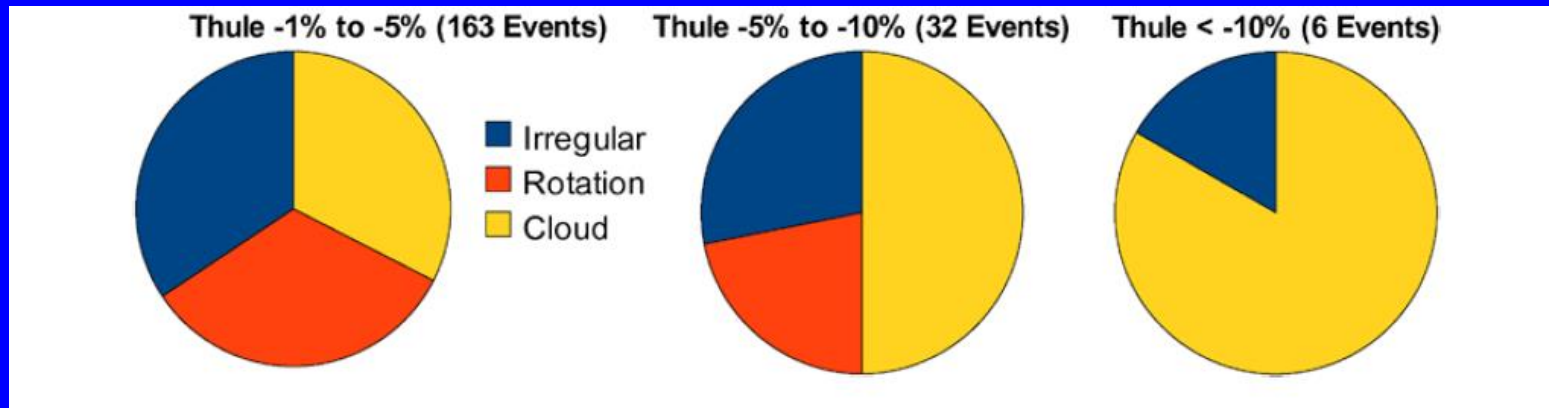
## Poor Correlations Between FD Size and Magnetic Cloud Diameter(a) or Axial Magnetic Field(B) (from Lepping Magnetic Cloud Fits)



Right hand figure: FD size vs.  $BVa^2$ , the parameterization suggested from a simple model of GCR transport into a MC based on the heat conduction equation developed by Wibberenz and Vanhoeffler (*Cane et al.*, 1995; *Vanhoeffler*, Master's thesis, 1996).

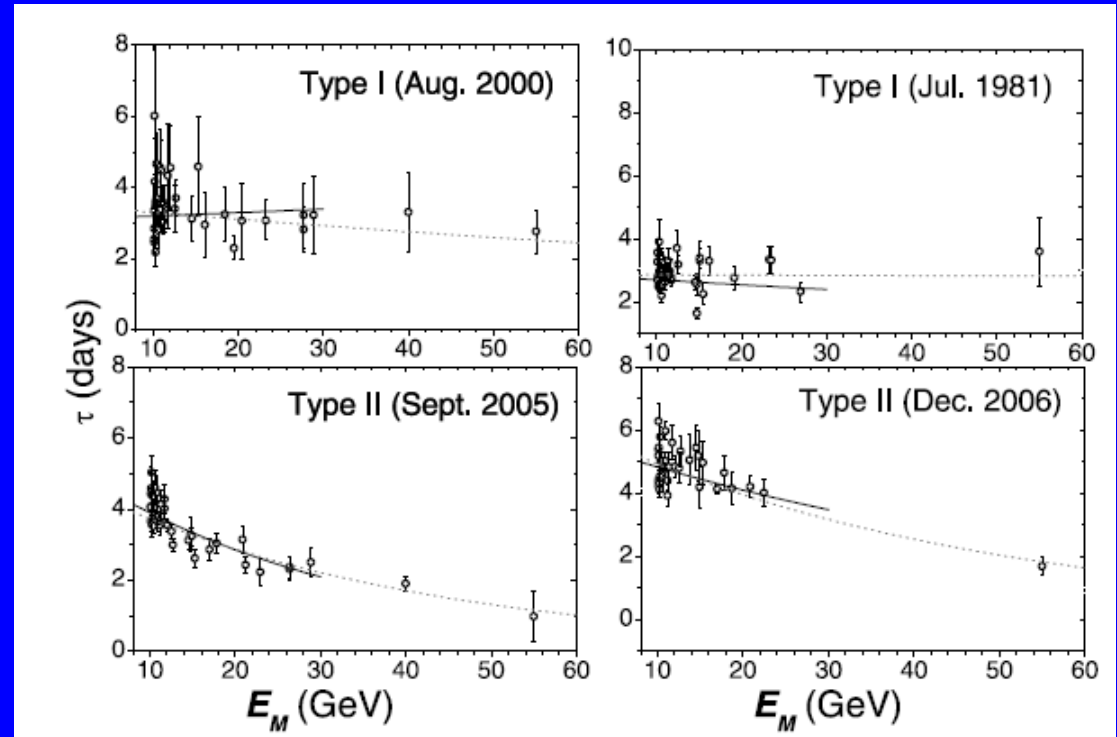
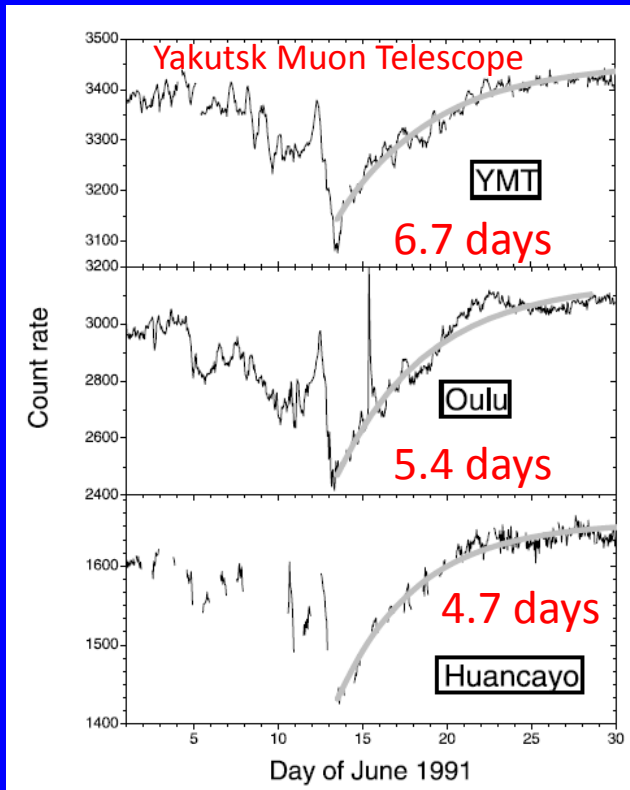
Note results do not take trajectory through the cloud into consideration.

# Distributions of ICME types Associated with Thule FDs of Different Size Ranges



Magnetic Clouds are more likely to be present as the FD size increases.

# Energy-Dependence of FD Recovery Time (*Usoskin et al., 2008*)



Type 1: No energy-dependence of recovery time

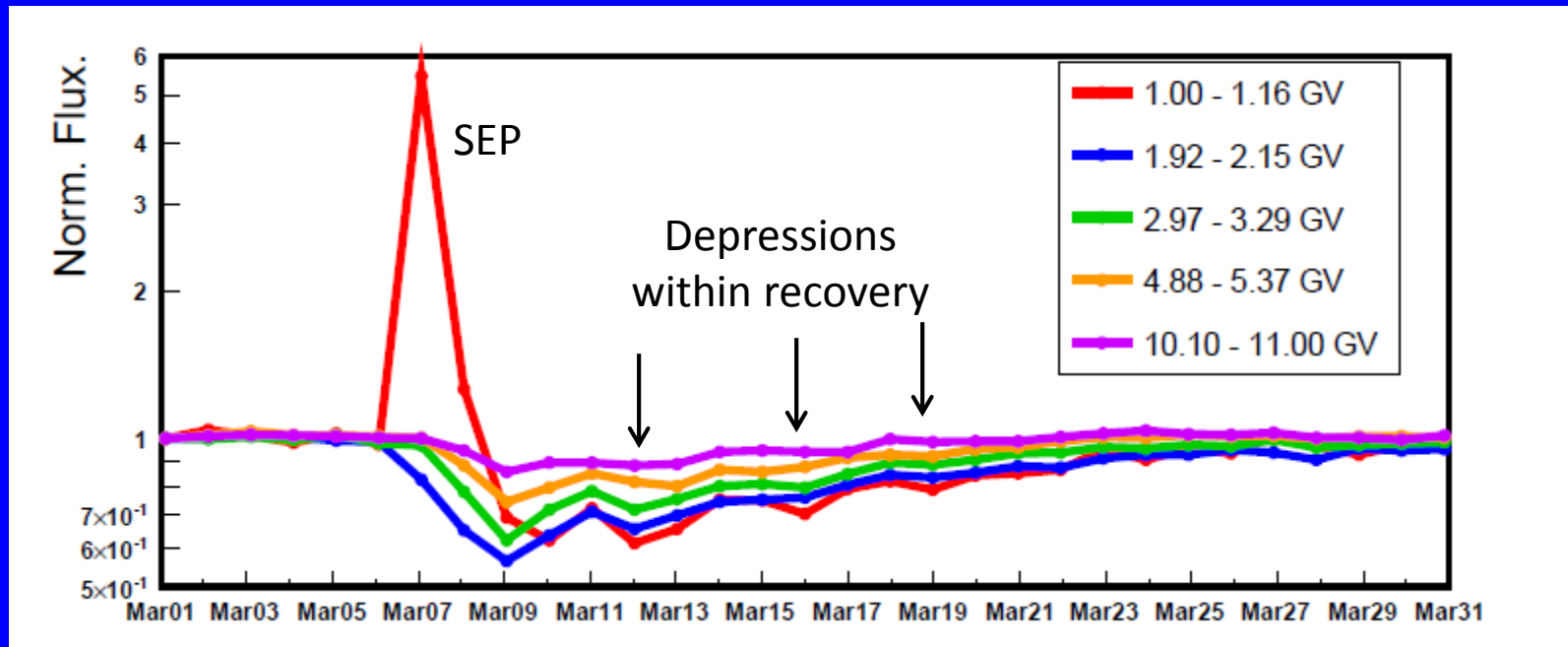
Type II: Energy-dependent recovery time.

“Recovery phase is determined by the effect of dissipation of the shock modulation” –

“Radial” departure – no energy dependence

“Longitudinal” departure – energy dependence

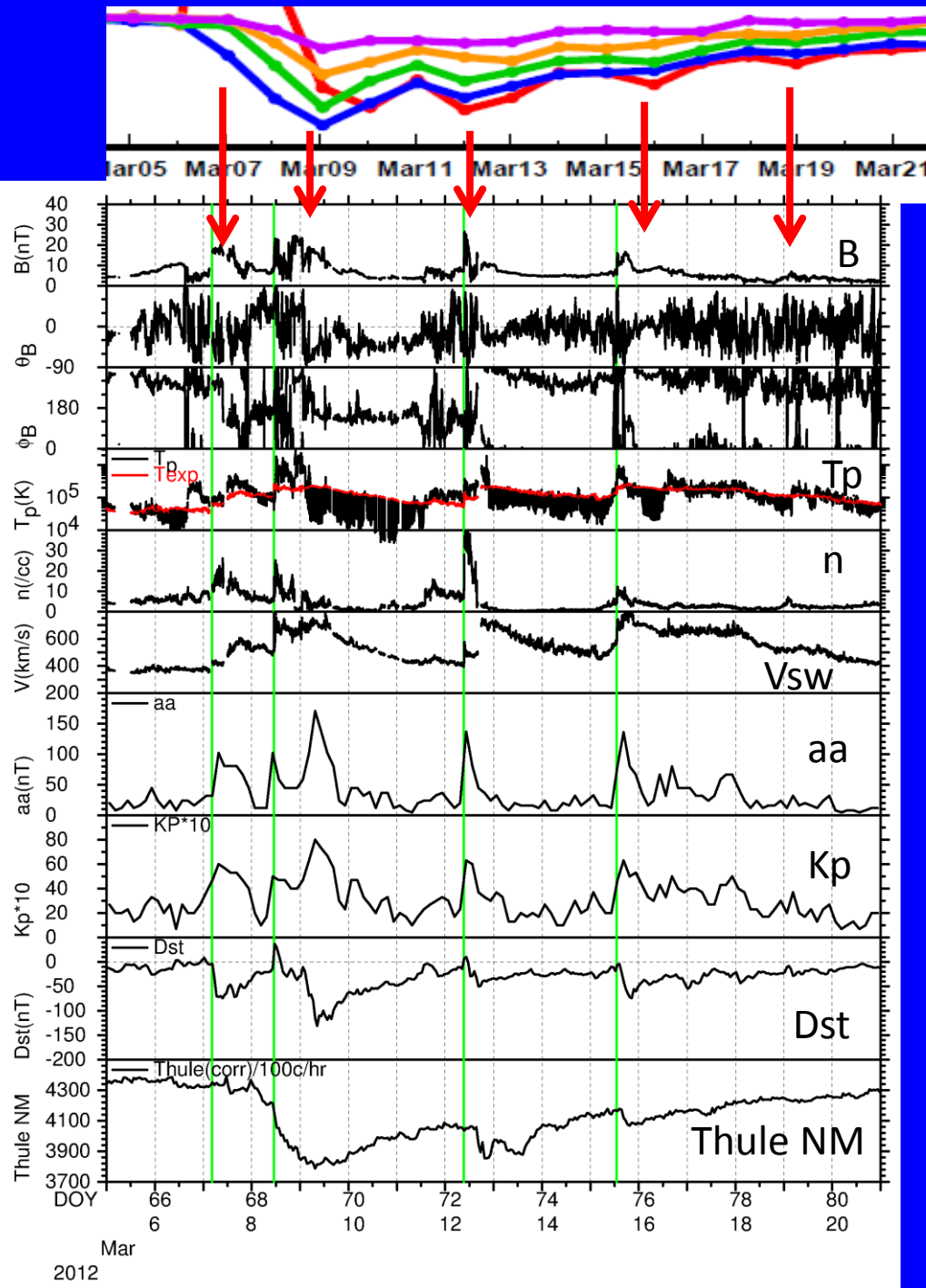
# AMS Observations (1-day Averages) of an SEP Event (March 7, 2012) and Forbush Decrease (*Consolandi et al., 2015*)



Clear rigidity-dependence of FD size

Why is the FD so extended?

Why are there additional depressions within the recovery?



Extended FD is due to a sequence of shocks and ICMEs.

Depressions within FD are subsidiary FDs associated with these structures, seen clearly by the Thule NM.

AMS data with  $\ll 1$  day resolution are required to study Fds in detail.

Associated geomagnetic storms are also evident.

## Summary

Spacecraft observations of GCRs during Forbush decreases complement those made by ground based observatories.

Features in the GCR intensity can be closely related to structures in the local solar wind observed by the same spacecraft.

Give a more global view of Fds.

AMS has the potential to contribute to Fd studies (e.g., study the rigidity dependence), but time resolutions  $\ll 1$  day would be useful.